BOLT BERANEK AND NEWMAN INC

CONSULTING • DEVELOPMENT • RESEARCH

Report No. 3208 NASA CR-144929

EXPLORATORY STUDY TO REDUCE FAN NOISE IN THE TEST SECTION OF THE NASA LANGLEY FULL-SCALE WIND TUNNEL

I.L. Vér
R.E. Hayden
M.M. Myles
B.E. Murray

December 1975

Submitted to:

Dr. James Sheiman
NASA Langley Research Center
Hampton, Virginia 23665
Mail Stop 404

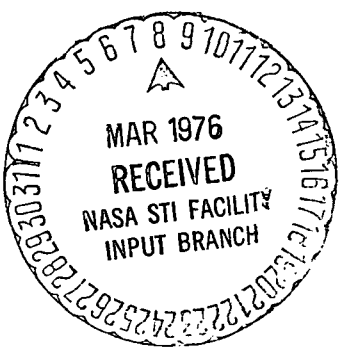

Report No. 3208 NASA CR-144929

EXPLORATORY STUDY TO REDUCE FAN NOISE IN THE TEST SECTION OF THE NASA LANGLEY FULL-SCALE WIND TUNNEL

I.L. Vér
R.E. Hayden
M.M. Myles
B.E. Murray

December 1975

Submitted by:

Bolt Beranek and Newman Inc.
50 Moulton Street
Cambridge, Massachusetts 02138

Submitted to:

Dr. James Sheiman
NASA Langley Research Center
Hampton, Virginia 23665
Mail Stop 404

SUMMARY

This report summarizes the results of work performed by Bolt Beranek and Newman Inc. (BBN) under Contract NAS1-13585 to identify feasible measures to reduce the intensity of the fan noise in the test section of the NASA Langley 30 ft × 60 ft subsonic wind tunnel.

First, field measurements were performed to document existing aerodynamic and acoustic conditions. The purpose of these experiments was to (1) obtain the "transfer function" between the sound power output of the fan and the sound pressure on the test platform, (2) evaluate the sound attenuation around the tunnel circuit, (3) measure simultaneously the flow profile and the turbulence spectrum of the inflow to the fan and the noise on the test platform, and (4) perform flow observations and listening in various parts of the tunnel to identify secondary noise sources.

Subsequently, these measured aerodynamic and acoustic data were used to predict (1) the relative contribution of the various major aerodynamic parameters to the total fan noise and (2) how the insertion of a dissipative silencer in the collector duct upstream of the fan would reduce both the fan noise in the test section and the maximum achievable tunnel speed.

These experimental and analytical studies led to the identification of promising noise control measures, and detailed recommendations were made on how to evaluate the expected benefits of these noise control measures via scale-model studies. The scale-model experiments, conducted by NASA personnel, are in progress.

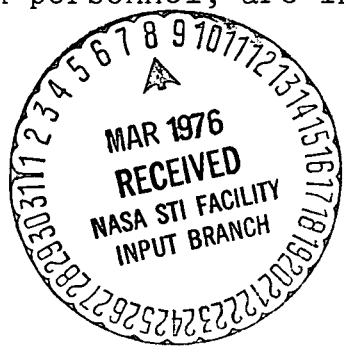

TABLE OF CONTENTS

TABLE OF CONTENTS *(Cont.)*

LIST OF FIGURES AND TABLES

LIST OF FIGURES AND TABLES *(Cont.)*

1. INTRODUCTION

The NASA Langley 30 ft × 60 ft subsonic wind tunnel was not designed originally to be used for acoustical measurements. A recent evaluation of the acoustical environment in the tunnel test section [1]* has indicated that both the reverberant buildup of the sound generated by the test object and the fan noise that enters the test section primarily via the collector interfere with the measurement of the direct sound field generated by the test object. Scale-model acoustical studies were undertaken [2] to optimize the spatial distribution of sound-absorbing treatment of the interior surfaces of the test section to reduce the reverberant buildup. As a result of these scale-model studies, sound-absorbing treatment was applied to selected surfaces of the test section. As predicted by the model studies, this treatment substantially reduced the reverberant buildup in the test section. However, the fan noise still interfered with the use of the tunnel for aeroacoustic studies.

Consequently, NASA requested Bolt Beranek and Newman Inc. to assist NASA personnel in identifying feasible measures to reduce the fan noise in the test section of the tunnel and thereby increase its usefulness for aeroacoustic research. The work performed in Phase I of contract NASI-13585 is summarized in this report.

*The numbers in brackets refer to references listed at the end of this letter report.

2. TECHNICAL DISCUSSION

The fan noise in the tunnel test section can be reduced by (1) reducing the noise output of the fan, (2) attenuating the fan noise along its path from the fan to the test section, or (3) a combination of the above two measures.

In addition to producing the required airflow, the fan also produces noise as an unwanted by-product. The fan noise is caused primarily by fluctuating lift forces on the blades, which result in local compression of the air. Even if the inflow to the fan were homogeneous and free of turbulence, noise would still be generated by vortex shedding and by the interaction of the turbulent boundary layer of the blades with the trailing edge of the fan blades. However, the inflow to the fan is distorted by the presence of the test platform and it is also highly turbulent along the perimeter of the collector. The intense turbulence is due to the mixing of the free jet with the surrounding stationary air in the open test section. Part of this thick shear layer is collected by the collector cowl and reaches the tip region of the fan blades. The fluctuations in the angle of attack produce fluctuating lift forces on the blade which, in turn, generate noise. The inhomogeneous inflow manifests itself in the blade passage tone and in its harmonics, while the random turbulent velocity fluctuations generate broadband random noise. The turbulent and distorted inflow and the trailing edge interaction and vortex shedding contribute substantially to the total noise signature of the fan. The fan noise in the test section can be reduced by lowering the sound power output of the fans by reducing the aerodynamic forcing function (i.e., reducing inflow distortion and turbulence), by reducing the blade response (i.e., blade sweep, porous edge, etc.) or by a suitable combination of these two measures.

However, the noise in the test section can also be reduced without lowering the noise output of the fan by attenuating the noise along its path from the fan to the test section. Fan noise can reach the test section via the direct path or via the long return leg. Since the direct path is short and a line of sight exists, while the return path is very long and has four 90° bands, the fan noise in the test section is controlled by the direct path. Accordingly, the noise in the test section can be reduced substantially by inserting a silencer into the collector duct upstream of the fans. If the sound attenuation of the silencer is not greater than the natural sound attenuation in the untreated return leg, the noise reduction in the test section is approximately the same as the sound attenuation of the silencer. However, the presence of the silencer will also change the inflow conditions to the fan. This changed inflow may, to a certain degree, decrease or increase the sound power output of the fan. If the silencer improves the homogeneity of the inflow, it also may render the fan more efficient and may partly compensate for the increased circuit resistance caused by its presence.

Naturally, both source and path noise control measures must not degrade the aerodynamic performance of the tunnel more than is tolerable. Accordingly, during the scale-model studies both the noise in the test section and the aerodynamic performance must be monitored simultaneously.

3. FIELD MEASUREMENTS AND OBSERVATIONS

BBN assisted NASA personnel in planning and carrying out a program of field measurements on the 14*th* and 15*th* of November 1974. The purpose of these field measurements was to obtain quantitative and qualitative information on the room acoustics and aeroacoustic properties of the Full-Scale Tunnel. The information needed for the conceptual design of promising noise control measures included: (1) the transfer function between the sound power output of the fan and the sound pressure on the test platform as a function of frequency, (2) the evaluation of the sound attenuation of the return leg of the tunnel as a function of frequency, (3) the simultaneous recording of the flow profile, the turbulence spectrum of the inflow to the fans, and the noise spectrum on the test platform, and, (4) the observation of flow patterns by tuft probes and careful listening to the noise generated by the fan and by other secondary noise sources.

3.1 Transfer Function

The most useful engineering formulas developed to predict fan noise given the sound power output of the fan as a function of requency with the propeller geometry, rpm, and the inflow conditions as variables. Since we were primarily interested in predicting the spectrum of the fan noise on the test platform, we needed the functional relationship between the sound power introduced into the tunnel at the fan location and the sound pressure produced by this induced sound power on the test platform. Fortunately, this relationship depended almost entirely on the tunnel geometry and on the absorption of the interior tunnel surfaces. Accordingly, the sought transfer function could be evaluated by placing a sound source of known calibrated sound power output at typical blade tip locations and monitoring the

sound pressure level spectrum that this calibrated source produced on the platform. In our tests, we attached a standard ILG source to hear the tip of one of the fan blades and recorded the sound pressure on the test platform for a number of different locations of the ILG source, ranging from the bottom to the top position. The transfer function $SPL_{PLATFORM} - PWL_{SOURCE}$ as plotted in Fig. 1 was found to be practically independent of frequency as well as source position (i.e., upside or down). In the graph, the octave band sound pressure level is referenced to 0.0002 μbar = $2 \times 10^{-5} N/m^2$ and the octave band sound power level to 10^{-12} W. Below 250 Hz, the ambient noise prevented the evaluation of the transfer function.

3.2 Sound Attenuation in the Return Leg of the Tunnel

Because of the closed loop, fan noise can enter the tunnel test section via both the short direct path and the long return path. Since the long return path provides a substantially higher sound attenuation than the shorter direct path, in steady state, the fan noise in the test section is controlled by the direct path, and the contribution of the indirect path is negligible. However, if one contemplates inserting an effective silencer into the collector duct upstream of the fans, which would substantially attenuate the noise reaching the test section through the direct path, the noise entering the test section through the indirect path sets a limit to the reduction of the noise in the test section. To avoid costly overdesign, the attenuation of the silencer should not be much higher than that of the return path. During our measurements, it was not practicable to block the path of the direct sound, and so there was no direct way to measure the sound attenuation along the indirect path. The information needed to estimate this attenuation was obtained indirectly from impulse response and steady state measurements, as outlined below.

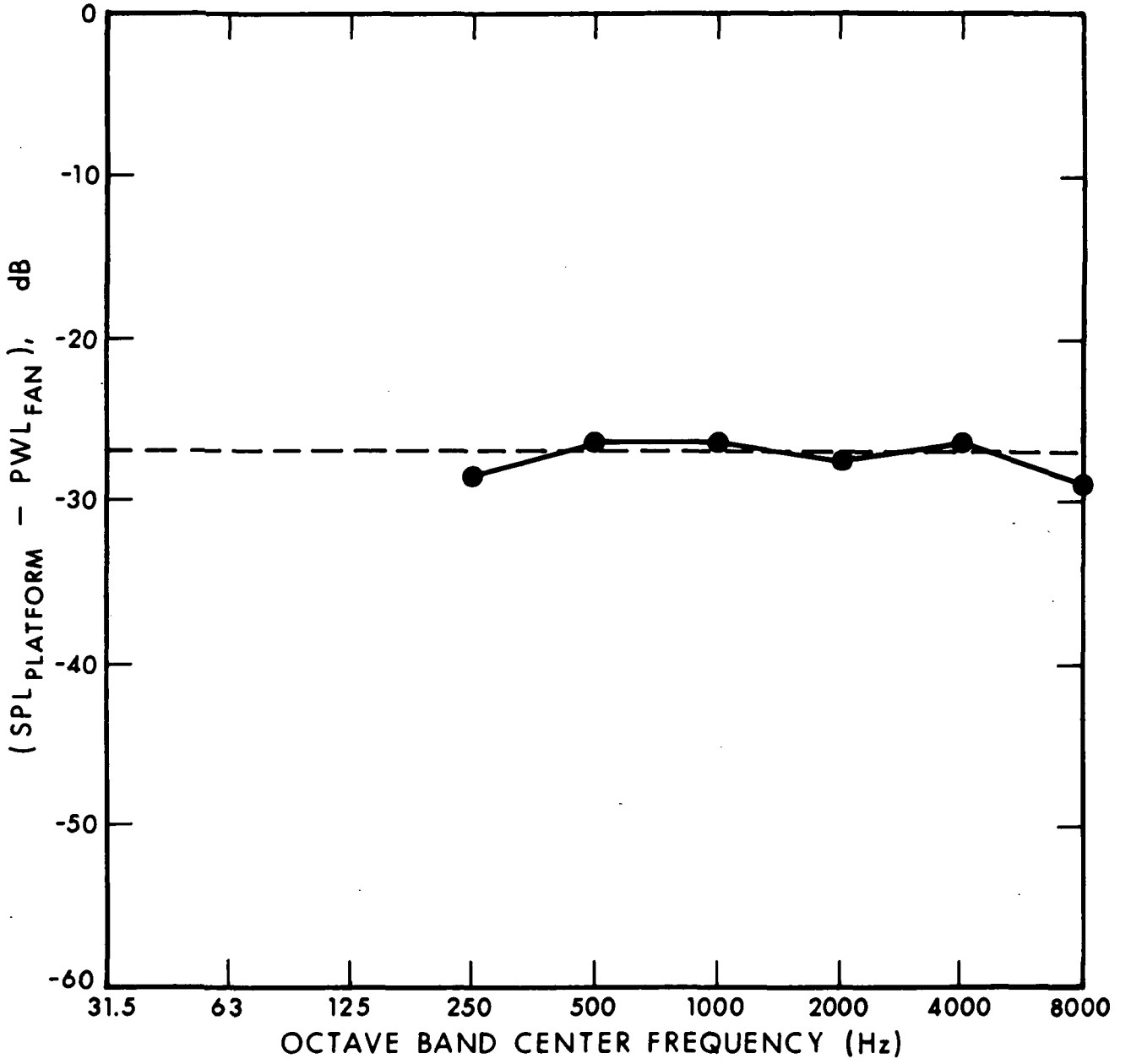

FIG. 1. MEASURED TRANSFER FUNCTION.

3.2.1 Impulse response method

A yachting cannon placed near the stationary fan blades served as a high-power impulsive noise source. The microphone was placed on the test platform, and the impulse response was recorded on magnetic tape. The recorded impulse response was played back, filtered in octave bands, and displayed on the screen of an oscilloscope or on the paper tape of a graphic level recorder. The sound pressure level vs time display of all impulse responses showed a double slope (see the trace of a typical screen photograph, Fig. 2). The initial faster rate of decay up to 0.6 sec was controlled by the energy fed into the test section via the short direct path. Approximately 0.6 sec after the cannon shot, the sound energy that traveled through the return leg of the tunnel entered the test section and fed energy into it. Accordingly, 0.6 sec after the cannon shot, the test section received sound energy through both the direct and indirect paths. The return leg of the tunnel had very little absorption and efficiently stored sound energy in its resonant modes, which fed energy into the test section. Accordingly, 0.6 sec after the cannon shot, the sound pressure level in the test section was controlled by the energy arriving through the nozzle, and the decay rate slowed down. Since the steady state sound pressure in the test section was made up of the superposition of an infinite number of impulse responses weighted in their amplitude according to the time dependence of the excitation, the difference in sound pressure level attributable to the direct and indirect path, respectively, could be well approximated by

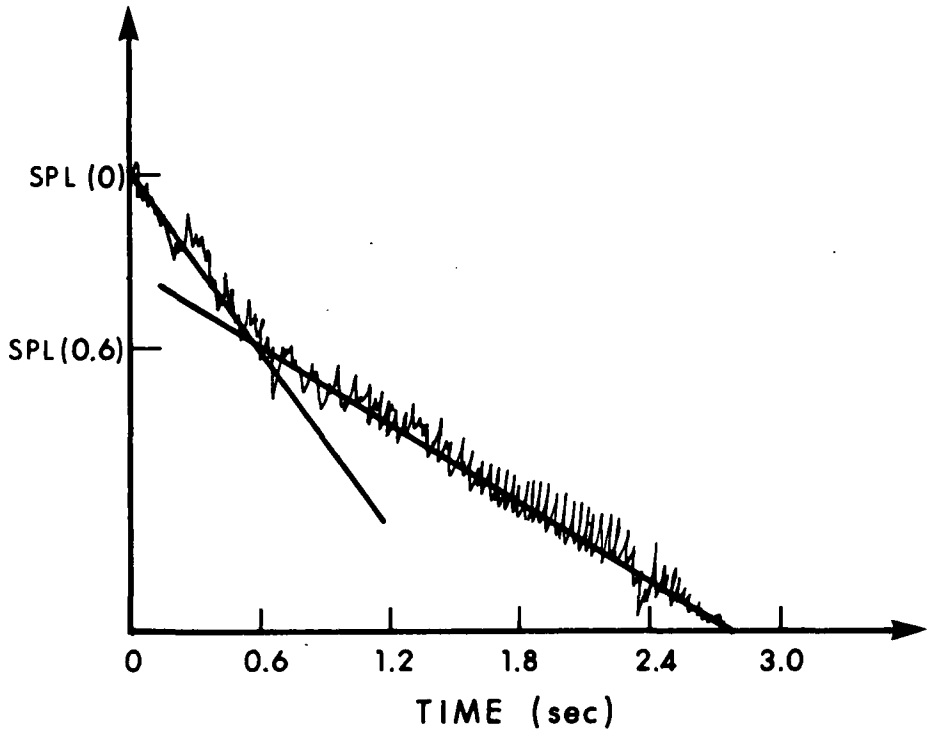

FIG. 2. TYPICAL IMPULSE RESPONSE CURVE

$$SPL_{dir} - SPL_{ind} \approx 10 \log \left[\int_0^{\infty} p^2(0) e^{-2\alpha_1 t} dt \right] - 10 \log \left[\int_{0.6}^{\infty} p^2(0.6) e^{-2\alpha_2 t} dt \right]$$

or

$$SPL_{dir} - SPL_{ind} \approx SPL(0) - SPL(0.6) - 10 \log \left(\frac{T_{R_2}}{T_{R_1}} \right) ,$$

where p(0) and SPL(0) are the sound pressure and the sound pressure level of the initial amplitude of the direct signal at the test platform, p(0.6) and SPL(0.6) are the sound pressure and the respective sound pressure level measured 0.6 sec after the arrival of the direct signal, T_{R_1} and T_{R_2} are the initial reverberation time, evaluated from the initial slope of the impulse response curve, and "tail end" reverberation time, evaluated from the second slope of the impulse response curve obtained 0.6 sec after the arrival of the direct signal.

The sound pressure levels SPL(0) and SPL(0.6) were obtained from the screen of the Spectral Dynamics Analyzer working in its transient capture mode. The reverberation times T_{R_1} and T_{R_2} were evaluated by playing the tapes backward and recording the traces on a General Radio Graphic Level Recorder whose pen motion was appropriately damped. The $SPL_{dir} - SPL_{ind}$ curves obtained by the above method are plotted in Fig. 3 as function of frequency indicating a loop attenuation of approximately 10 dB.

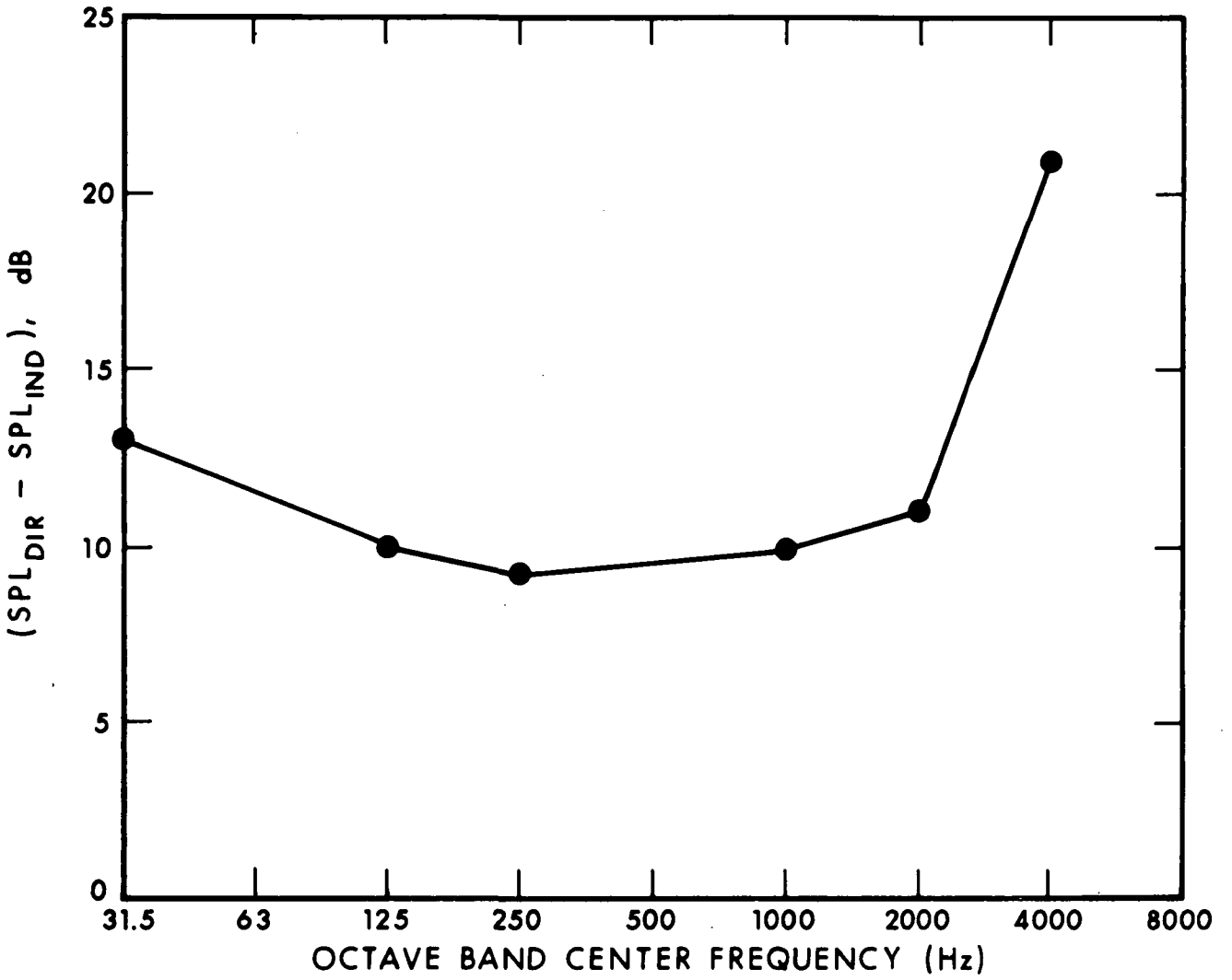

FIG. 3. SOUND ATTENUATION IN THE RETURN LEG.

3.2.2 Steady-state method

The spatial distribution of the sound pressure for steady-state conditions gives an additional indication for the sound attenuation along the return leg of the tunnel. The tunnel fans, operating at a low rpm, served as a noise source. The sound pressure level was recorded at eight different locations along the tunnel circuit. As shown in Fig. 4, Position 1 is near the nozzle opening at the bridge while Position 8 is just downstream of the drive section. The 30-sec-long samples recorded at these locations were played back and analyzed in octave bands. Subsequently, all SPL vs position curves were normalized to their respective value measured at Position 1. Figure 5 is a plot of these normalized SPL vs position curves with the frequency as parameter. Because of the close clustering of the data points, the symbols are not connected by lines.

At Position 4, which corresponds roughly to a half-loop length, the data points cluster around -5 dB. This result agrees qualitatively with the approximately 10-dB loop attenuation obtained from the more accurate impulse method.

3.3 Inflow Conditions

To estimate the level of fan noise, the inflow conditions and blade configuration must be known. The inflow conditions were studied experimentally at an air speed corresponding to Tunnel Point 10. The mean flow velocity profile has been measured by traversing a probe just upstream of the west fan from the wall up to 5 ft toward the center line of the passage. Traverses were made in both the upper and lower part of the west collector duct. Velocity profiles obtained during these traverses were used to produce the axial velcoity profile shown in Fig. 6. The marked

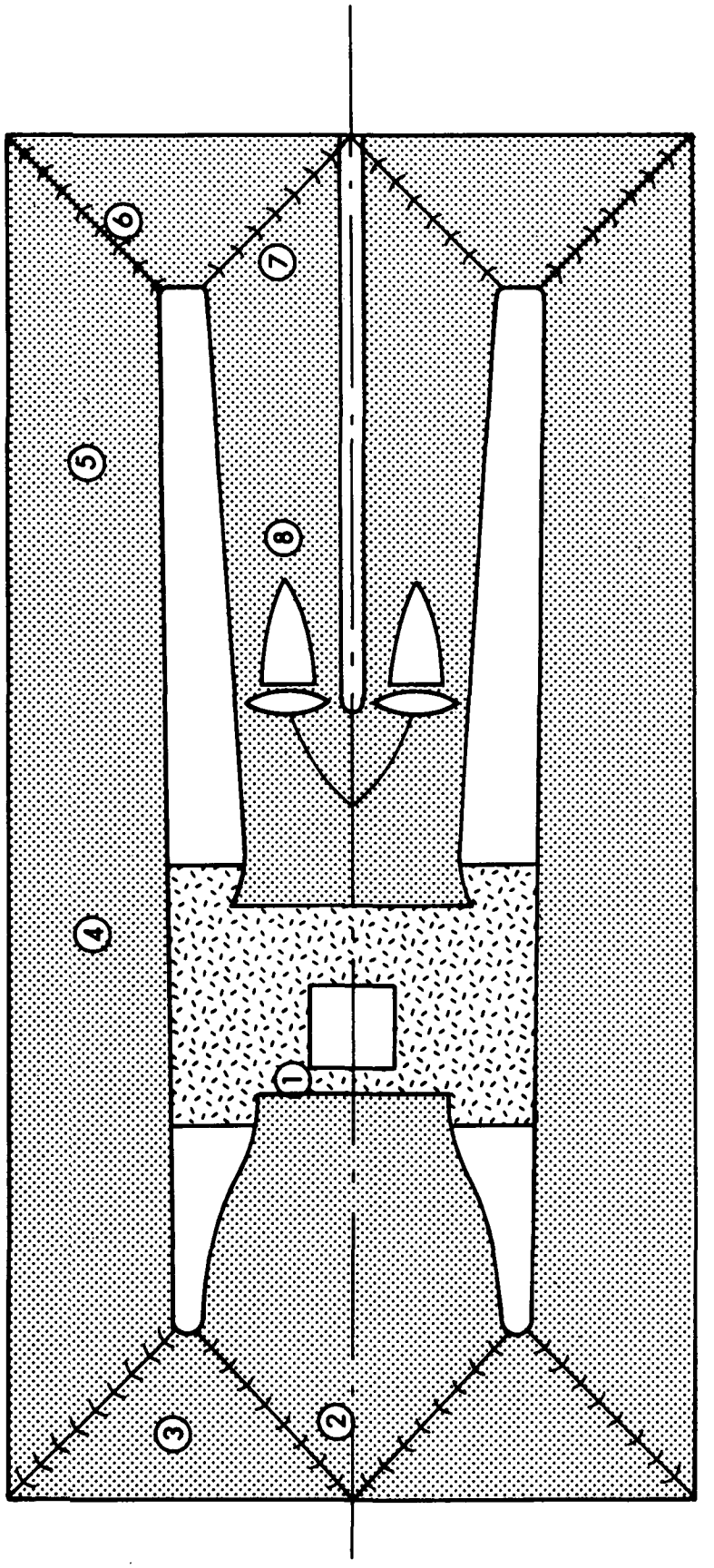

FIG. 4. MICROPHONE POSITIONS FOR STEADY-STATE TEST.

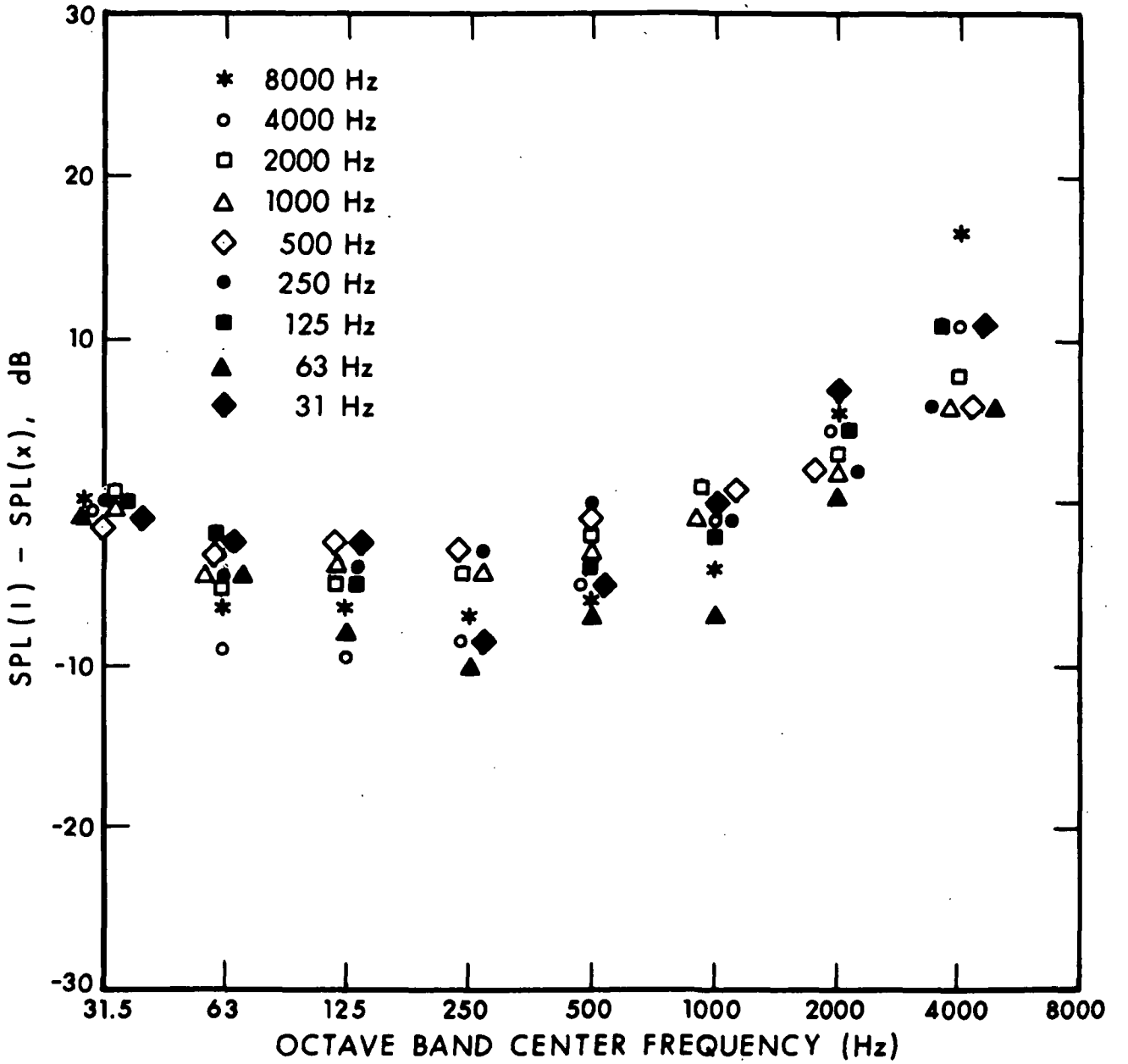

FIG. 5. SPATIAL DISTRIBUTION OF THE SOUND AROUND THE TUNNEL CIRCUIT LEVELS ARE NORMALIZED TO THOSE MEASURED IN THE TEST SECTION (POS.1) (SEE FIG. 4 FOR POSITIONS).

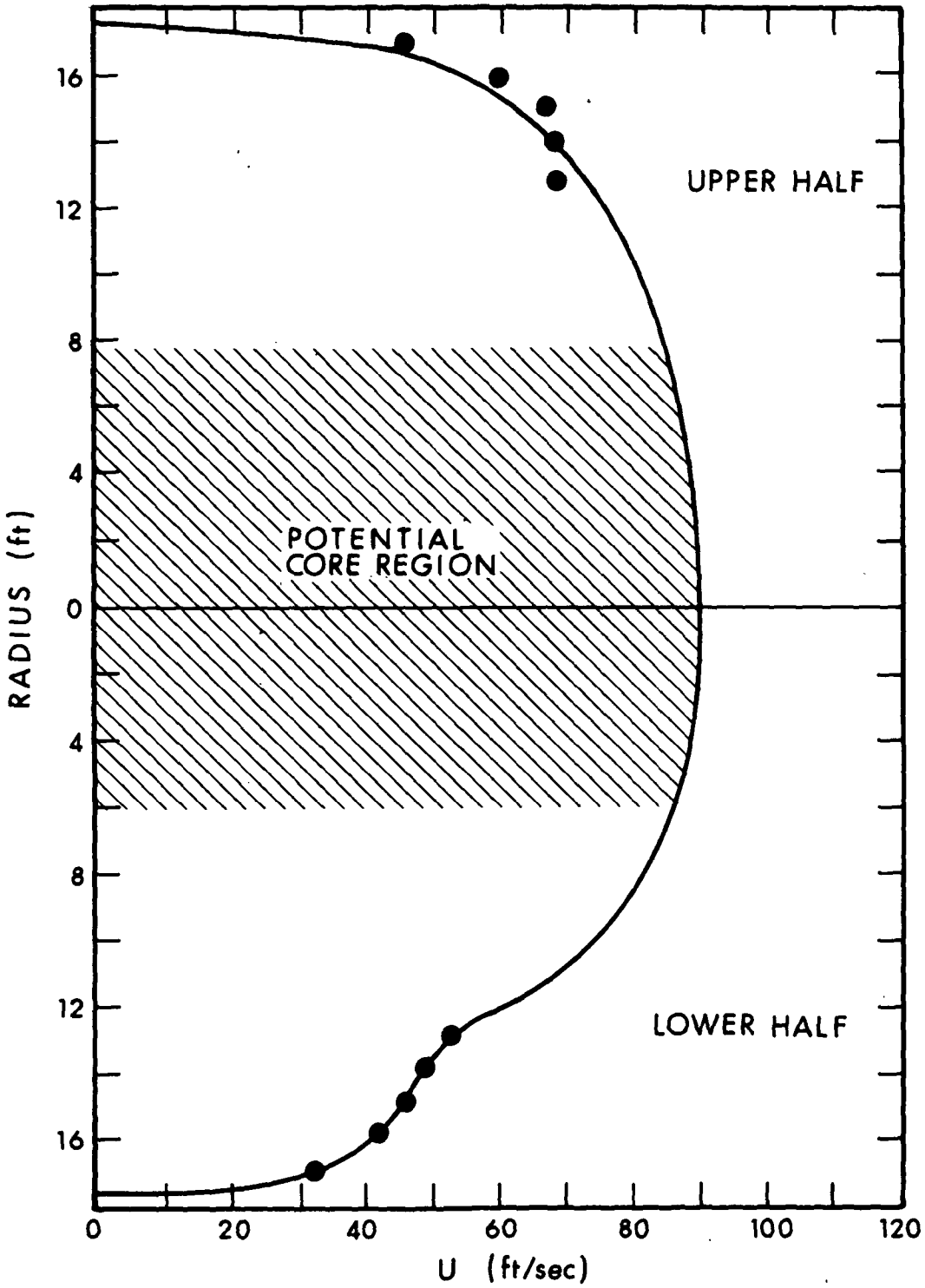

FIG. 6. AXIAL FLOW VELOCITY VS RADIUS, TUNNEL POINT 10.

velocity deficiency at the lower part of the collector duct is caused by the test platform and balance building, which effectively blocked the flow in the lower region of the test section.

The inflow turbulence was measured with a hot wire anemometer. The overall inflow turbulence was found to be 0.1 times the local mean axial velcoity in the upper part of the collector duct and 0.2 times the local mean axial velocity in the lower part. These correspond roughly to 6.5 ft/sec rms velocity in the upper part of the collector duct and 9 ft/sec in the lower part. For the prediction of turbulence ingestion noise, an average of 7 ft/sec was assumed for the full circumference. At Tunnel Point 10 and at 15-ft radius, the mean air velocity over the blade is 265 ft/sec, yielding 2.6% relative turbulence in this blade region.

Spectrum analysis of all the anemometer signals showed that the turbulence spectrum decreases with increasing frequency. The rate of decrease was found to be 3 dB/octaves if analyzed in constant percentage bandwidth (i.e., octave bands). Accordingly, it is reasonable to assume that the overall turbulence level of 7 ft/sec rms is, for all practical purposes, well approximated by the rms-based combination of the turbulence levels in the 16-Hz, 31-Hz, 63-Hz, and 125-Hz center frequency octave bands. The wave number k at each center frequency f_c was calculated by using the relative airspeed of U = 265 ft/sec as $k = 2\pi f_c/U$. Table 1 summarizes the results of these calculations.

TABLE 1. SPECTRAL DISTRIBUTION OF THE TURBULENT VELOCITY FLUCTUATIONS (Tunnel Point 10, 15-ft Radius).

Octave Band Center Frequency	16 Hz	31.5 Hz	63 Hz	125 Hz
Wave Number (ft^{-1})	0.38	0.72	1.44	2.88
rms Turbulent Velocity (ft/sec)	3.73	1.87	0.93	0.47

3.4 Qualitative Observations

In addition to gathering quantitative data during the 1974 field measurements, BBN and NASA personnel made a number of qualitative observations that provided insight into the noise generation processes. These observations included:

- Tuft probes over the mouth of the collector duct indicated the existence of an approximately 5- to 6-ft-thick highly turbulent layer around the entire perimeter of the collector duct. This results from the open test section where the free jet gets mixed with the surrounding stationary air, producing a highly turbulent shear layer. The conservation of mass in the test section requires that a part of this shear layer enters the collector duct. Except for a short arc of travel near the center line of the test section, the tip of the fan blades must operate in this highly turbulent shear layer.
- After carefully listening to the fan noise and correlating the visual and acoustical phenomena, we observed that an impulsive sound is generated each time a fan blade enters the lower part of the collector duct where a flow deficiency exists because of the blockage of the test platform. It is likely that the blade loading changes rapidly at this instant or that the blade tip goes into stall.

- Careful listening to the fan noise at low rpm revealed that vortex shedding from the trailing edge is an important contributor to the fan noise.
- Listening to the noise on the bridge just outside of the jet confirmed the existence of some low-intensity high-frequency noise of pure tone character. This noise is generated by the flow interacting with the regular perforations of the sound-absorbing panel covering the test platform. The sound power generated by this process is very small compared with that generated by the fan. However, in scale-model studies where microphones may be located near these surfaces, the noise may be of sufficiently high level to interfere with the measurement of low-level aeroacoustic signals generated by a small model.
- Through careful listening to the noise in the test section at Tunnel Point 10, we discovered that a number of tunnel structures were rattling and thereby generating noise of a semiperiodic nature, which was not masked by the fan noise.

Rattling was observed at:

The railing at the lower part of the collector cowl, which is constructed of pipe. As a safety measure, a strong wire cable is pulled through the pipes. The rattling noise is caused by the vibration of this wire cable. Enclosing the wire cable in a soft packaging would probably solve this problem.

One of the acoustic panels on the south wall of the test section above the collector cowl.

Certain light fixtures in the upper part of the test section.

Though the sound power output of these rattling surfaces is small compared with that of the driving fans, they could become significant if their characteristic frequencies coincide with low-level aerodynamic pure tones generated by a small model, especially after fan noise has been reduced appreciably.

4. AERODYNAMIC NOISE ANALYSIS OF THE DRIVING FANS

Calculations were performed to estimate the contributions of trailing edge turbulent boundary layer noise, the trailing edge vortex noise, the stall noise, and the turbulence ingestion noise to the noise levels measured on the test platform at Tunnel Point 10. Figure 7 presents the results of the aerodynamic noise calculations for the four mechanisms studied and compares them with the measured platform noise levels reported in Ref. 1.

The predicted trailing edge turbulent boundary layer noise and turbulence ingestion noise agree reasonably well with the measured total levels. However, the stall noise may be significantly lower than predicted because the calculation included only the periodic component of the forcing function. There is clearly some broadband noise associated with stall. To predict this noise would, however, require a more detailed data base and more extensive calculation. The predicted trailing edge vortex noise is more predominant than is seen in practice, possibly because the low-frequency turbulence ingestion breaks up the coherent behavior of trailing edge vortices. Additional effects that tend to reduce the vortex shedding strength include high tip loading and surface roughness.

The method of predicting the contribution of the various sources of fan noise to noise in the tunnel test section is summarized below.

4.1 Operating Conditions of the Fan

In our aerodynamic noise analysis, we predicted the noise generated over the upper 75% of the rotation and noise generated over the lower 25% of rotation separately. From the blade details supplied by NASA, the angle of attack of the blade was calculated

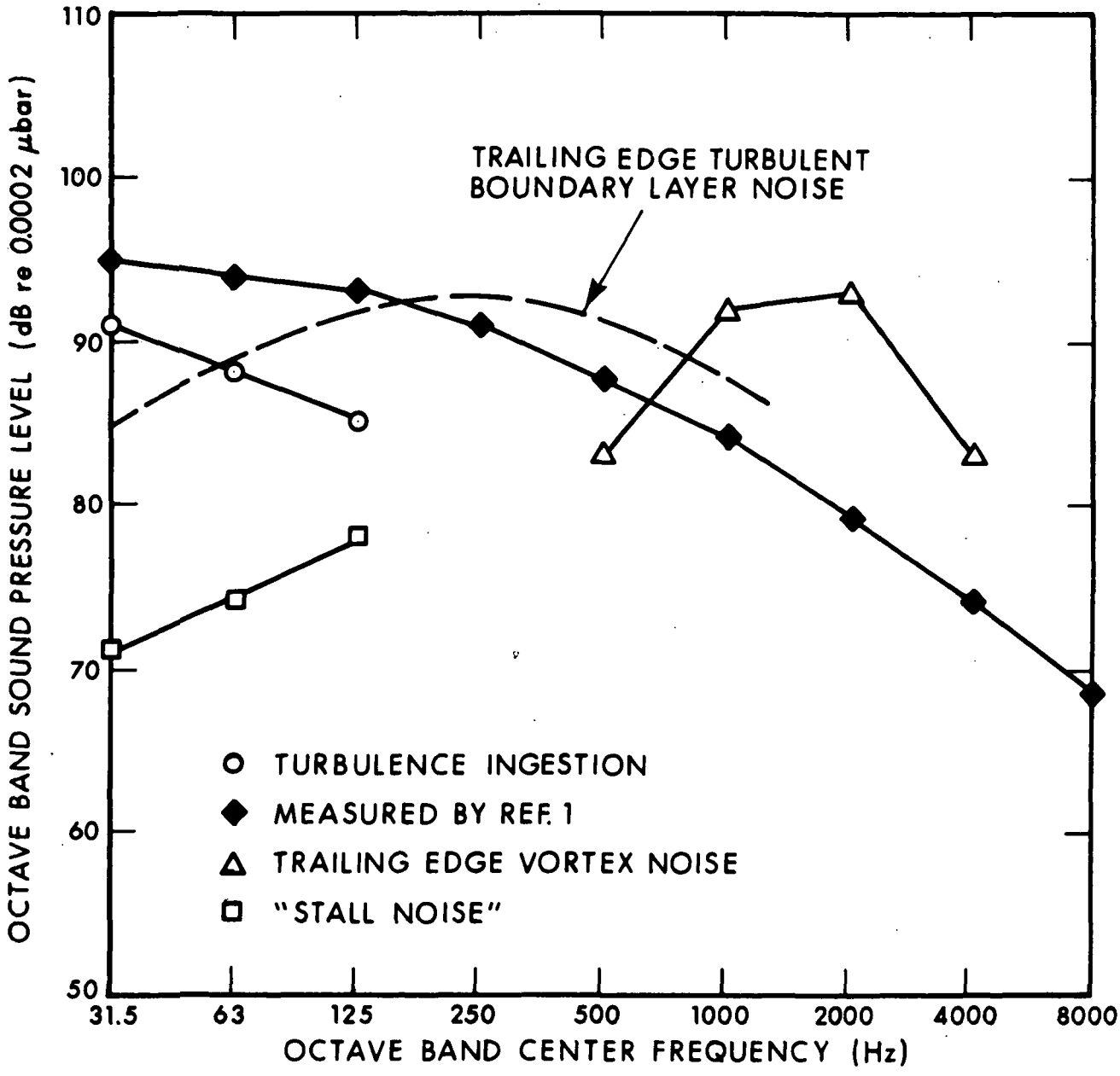

FIG. 7. MEASURED AND PREDICTED FAN NOISE IN THE TEST SECTION, TUNNEL POINT 10 (165 rpm).

together with the relative air velocity over the top 75% circumference for nine radial segments. The severe velocity deficit around the lower part of the arc had not been studied sufficiently to make an accurate assessment of the conditions in this area. Consequently, only a gross airfoil analysis was conducted over the outer 5 ft of blade span.

Figure 8 shows the calculated operating conditions for the blades over the upper 75% of rotation at 165 rpm, corresponding to Tunnel Point 10. Note that the blade is close to stall in the tip region.

4.2 Prediction of the Trailing Edge Turbulence Noise

The sound power level generated by the turbulent boundary layer at the trailing edge is

$$PWL \sim \log \frac{\rho U_m^6 \delta w}{12\pi c^3} \quad ,$$

where ρ = density of air, U_m = air velocity over the blade, δ = boundary layer thickness at the trailing edge, w = wetted span of the trailing edge, and c = speed of sound.

First, we found nine radial blade segments across which the change in air velocity would produce an approximately 3-dB change in sound power level. For each of these nine segments, the turbulent boundary layer thickness was estimated as 1/8*th* of the boundary layer displacement thickness. For the purposes of these calculations, the displacement thickness was taken as 6% of the mean chord of the blade segment. The turbulent boundary layer is thicker near the tip because of the proximity to stall. Accordingly, the turbulent boundary layer thickness calculated with the above method was doubled in this region.

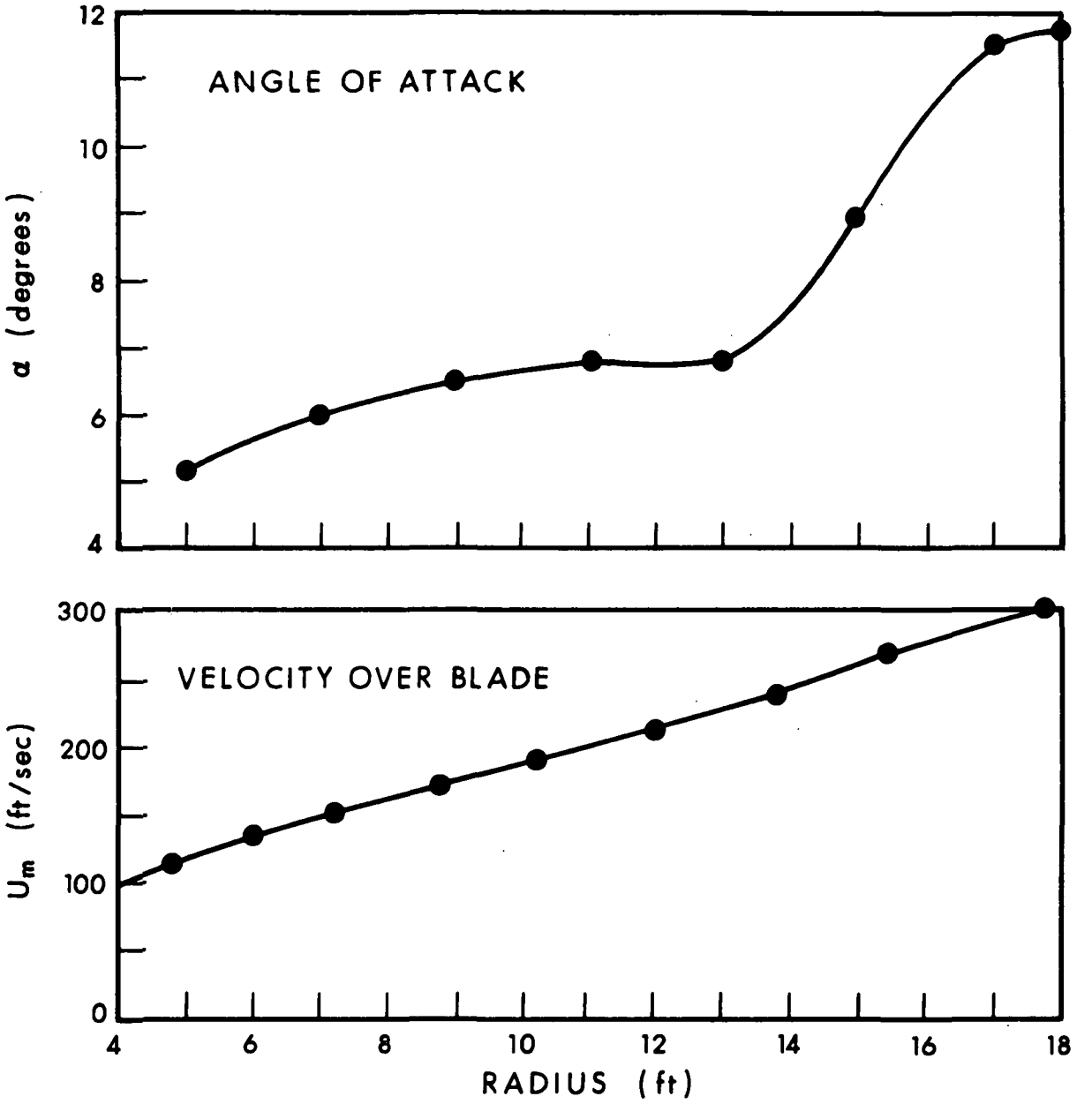

FIG. 8. BLADE OPERATIONAL CHARACTERISTICS TUNNEL POINT 10 (165 rpm), UPPER PART.

The parameters δ, w, and U_m^6 calculated for each segment were applied respectively to the empirical graph, yielding the normalized spectrum for an airfoil given in Fig. 9 [3]. First, the sound power levels were thus calculated in 1/3-octave bands for each segment, and then the total blade trailing edge noise was computed for all segments in octave bands for all eight blades over the top 75% rotation. The power levels were then converted to sound pressure levels on the test platform by taking the experimental transfer function shown in Fig. 1. The result is plotted in the summary graph of Fig. 7 which also includes the actual sound pressure levels on the platform at Tunnel Point 10 as measured by Ref. 1.

4.3 Trailing Edge Vortex Noise

The trailing edge vortex noise was calculated by using the same radial segments used for the turbulent boundary layer noise. First, the total displacement thickness at the trailing edge was computed for each segment. Using this result in conjunction with the respective span and U_m^6 values, we evaluated the trailing edge noise from the empirical data given in Fig. 10, taken from Ref. 3.

The overall level of vortex noise was determined for each segment together with the wake Strouhal number corresponding to the spectrum peak. The sound power levels at the peak frequencies for each segment were combined and converted into octave bands. The result is shown in Fig. 7.

4.4 Stall-Generated Noise

It is apparent from Fig. 8 that the blade tip stalls or approaches stall when it passes through the lowest quadrant of rotation. A gross analysis was made of the conditions that exist over

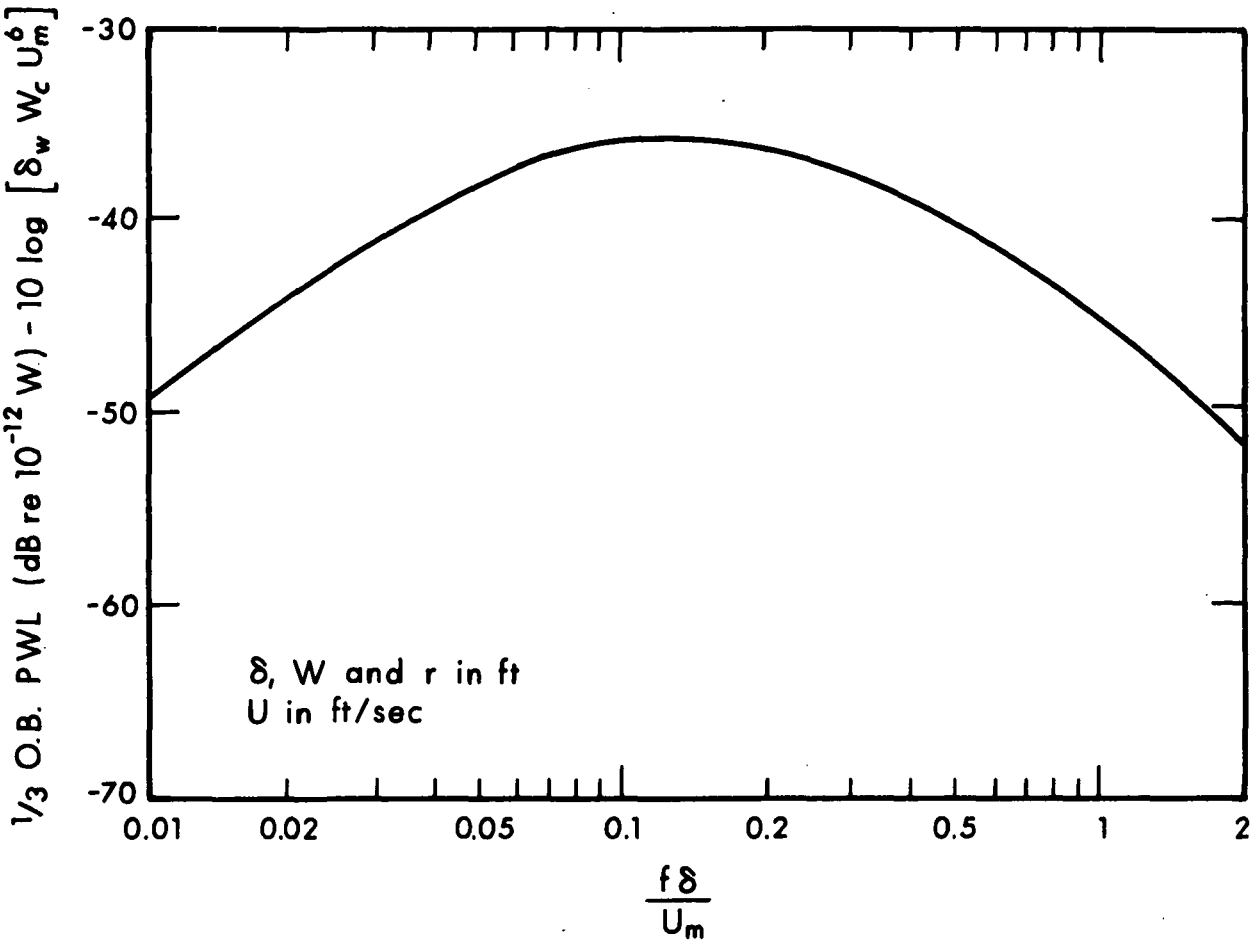

FIG. 9. NORMALIZED 1/3-OCTAVE BAND SPECTRA OF TRAILING EDGE NOISE (FROM REF. 3).

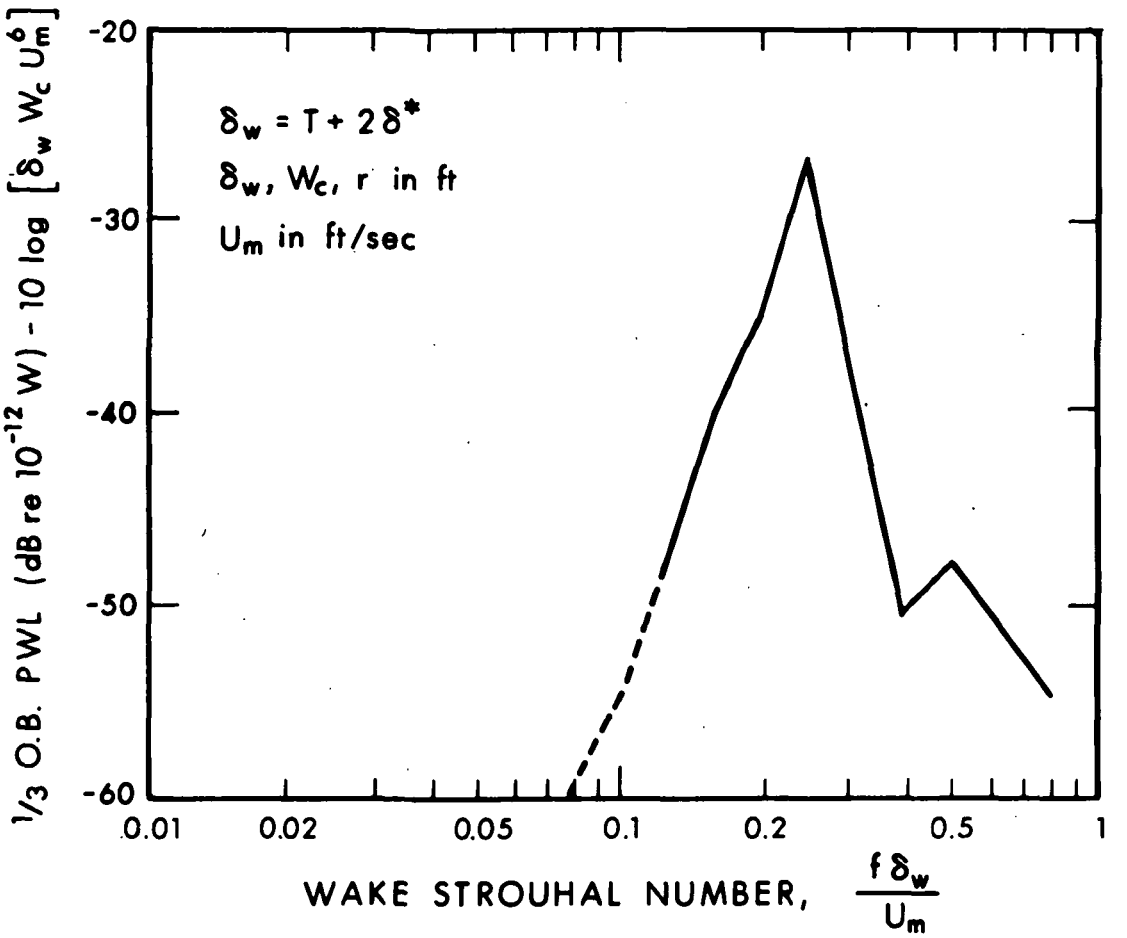

FIG. 10. NORMALIZED 1/3-OCTAVE BAND SPECTRUM OF WAKE-GENERATED NOISE (FROM REF. 3).

the outer 5 ft of span. Using the assumed velocity profile shown in Fig. 3, we calculated the blade angle of attack for the blade section at 15-ft radius at 9 angular positions 11.25° apart around the lower portion of the arc. Then, using the lift curve of the Clark Y airfoil, we calculated the fluctuating lift force on the outer 5 ft of span. This result is presented in Fig. 11, which shows that as one blade leaves the low-velocity area, another enters. The overall lift force fluctuation is thus similar to a fully rectified sine wave.

After determining the magnitude of the lift force at the fundamental blade passage rate and the time variation of the total blade force, we calculated the amplitude of the harmonics up to the 8*th* by Fourier analysis. The sound power level attributable for the fundamental and the harmonics was calculated, using the expression:

$$W = \frac{\omega^2 \overline{F}^2}{12\pi\rho c^3} \quad ,$$

where $\omega = 2\pi f$ is circular frequency of the blade passage, $\overline{F}$ = total blade force, ρ = density of air, and c = speed of sound in air.

These levels were then summed into octave bands, and the result is presented in Fig. 7.

4.5 Turbulence Ingestion Noise

We calculated the turbulence ingestion noise over the full 360° of blade rotation, using the average data for the outer 5 ft of blade span as given in Table 1. The effective dynamic lift coefficient for the specific turbulent inflow conditions (Table 1) was evaluated from Fig. 12, taken from Ref. 3. The 0.5 aspect

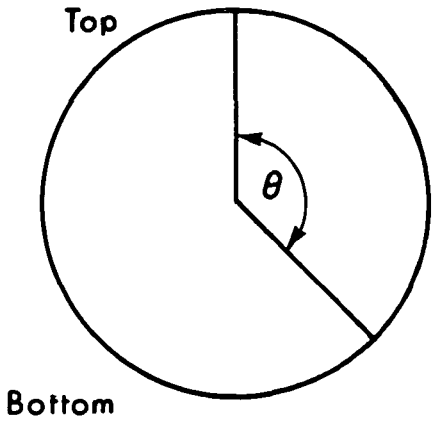

CONVENTION FOR BLADE POS.

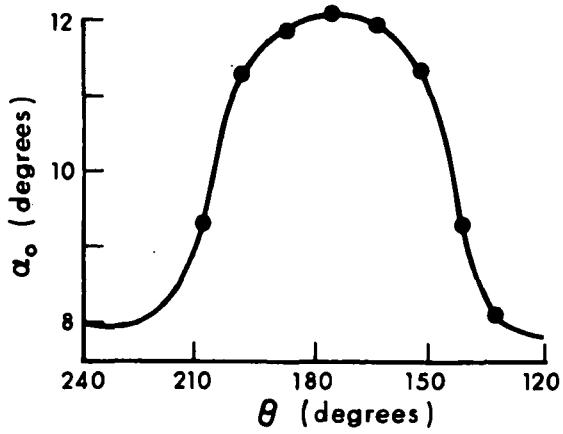

ANGLE OF ATTACK vs. POS.

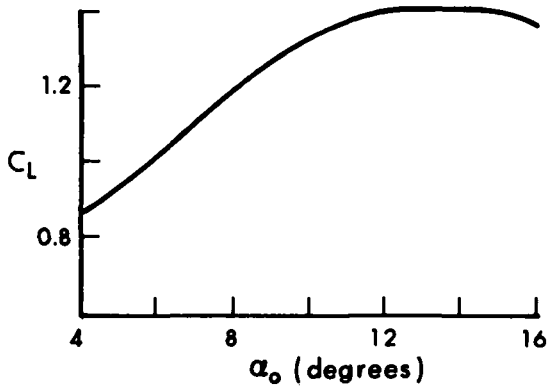

CLARK Y LIFT CURVE

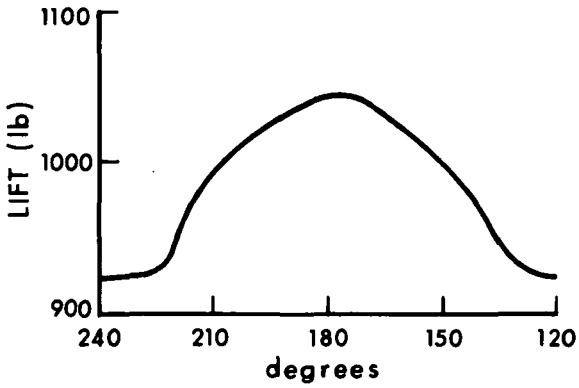

LIFT vs. POSITION

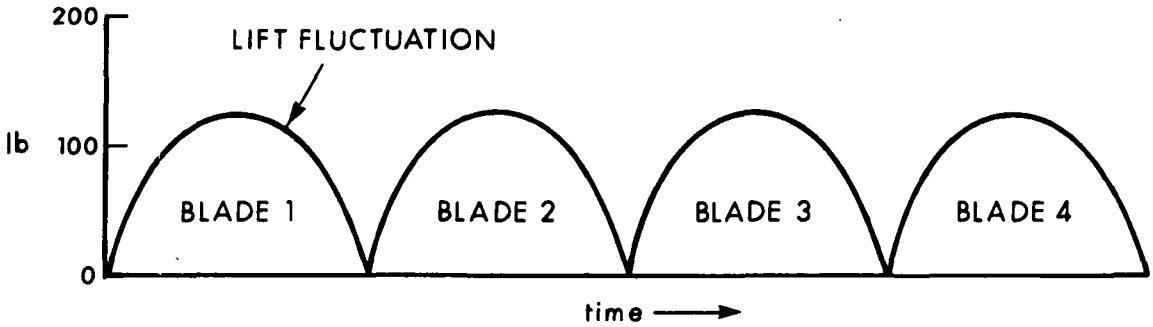

FIG. 11: LIFT FLUCTUATIONS DUE TO INFLOW INHOMOGENEITY.

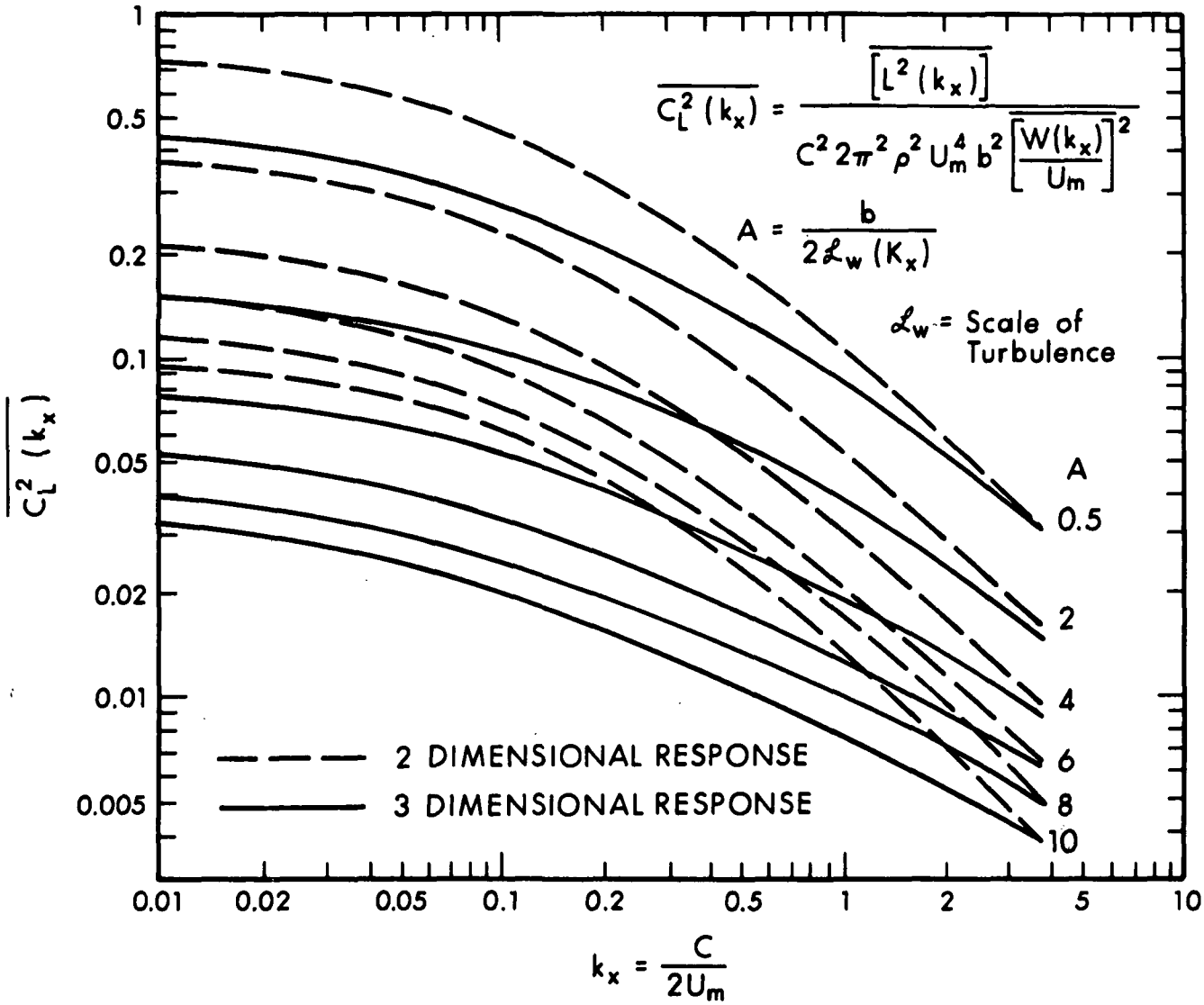

FIG. 12. LIFT RESPONSE OF FINITE SPAN AIRFOILS IN 2- AND 3-DIMENSIONAL INFLOWS (FROM REF. 3).

ratio and two-dimensional curve was taken as representative for our case. This yields the $\overline{C}_L^2$ values given in Table 2.

TABLE 2. EFFECTIVE LIFT COEFFICIENT AS A FUNCTION OF FREQUENCY.

Octave Band Center Frequency	16 Hz	31.5 Hz	63 Hz	125 Hz
$\overline{C}_L^2$	0.24	0.15	0.07	0.035

Inserting the above values of $\overline{C}_L^2$ into the equation below yields the fluctuating force on the outer 5 ft of the blade span as

$$\overline{F}^2 = \overline{C}_L^2 \{2\pi^2\rho^2 U_m^4 b^2 \ell_c^2 (v/U_m)^2\} \quad ,$$

where b = blade span, ℓ_c = blade chord, U_m = the air velocity over the blade, and v = rms turbulence velocity. The sound power generated was calculated in each octave band by inserting the above value $\overline{F}^2$ into the equation

$$W = \frac{\omega^2 \overline{F}^2}{12\pi\rho c^3} \quad .$$

The sound pressure level on the test platform, which is attributable to the turbulence ingestion, was then obtained by using the transfer function given in Fig. 1.* The levels obtained are given in Table 3 and are also plotted in Fig. 7.

*It should be noted that the same transfer function was used to relate sound power generated by other mechanisms to the sound pressure level they produce on the test platform.

TABLE 3. ESTIMATED OCTAVE BAND SPECTRUM OF THE PLATFORM NOISE DUE TO TURBULENCE INGESTION.

Octave Band Center Frequency	16 Hz	31.5 Hz	63 Hz	125 Hz
$SPL_{platform}$, dB re 0.0002 μbar	93	91	87	85

5. PRESSURE DROP AND ATTENUATION OF SILENCERS

The fan noise in the tunnel test section can be reduced substantially by inserting a parallel baffle-type silencer into the collector duct upstream of the driving fans. We have studied both the pressure drop and the sound attenuation achieved by the insertion of such silencers. The conclusions of these studies are summarized below.

5.1 Pressure Drop Prediction

We have developed formulas based on the measured drag coefficient [4] of a streamlined silencer baffle to calculate the percentage open area of the silencer treatment needed to assure that the pressure drop across the silencer does not exceed 8% of the dynamic pressure in the tunnel test section. This maximum pressure drop would correspond to a 10% decrease in the maximal airspeed achievable with the present drive system. These calculations have been reported earlier in our Progress Report No. 1, dated 18 November 1974. A summary of these calculations is given in Appendix A.

Equation 9 of Appendix A gives the needed minimum open area POA_{min} by

$$POA_{min} \approx 100 \left(1 - \frac{1}{2 + \frac{C_D S_0}{0.08 \ell_0 w}} \right) ,$$

where $C_D = 0.0152$ is the measured drag coefficient, $\ell_0 = 5.85$ ft is the edge length of the sample panel, $S_0 = 29.1$ ft^2 is the surface area of the sample panel, and w = width of the baffle. With these particular values, Eq. 9 reduces to

$$POA_{min} \simeq 100 \left(1 - \frac{1}{2 + \frac{11.34}{w}} \right) ,$$

where W is the panel thickness in inches. Evaluating the above equation for w = 4 in. and w = 8 in., we obtain an open area requirement of 79% and 71%, respectively. With these panel thicknesses and open areas, the distance between the face of two neighboring parallel baffles must be at least 16 in. and 19.6 in., respectively.

5.2 Prediction of Sound Attenuation

The results of the pressure drop calculations led us to select two silencer configurations for acoustical studies. Each of the silencers consists of 66-in.-long parallel baffles. Configuration 1 has 4-in.-thick baffles and is 79% open, while Configuration 2 has 8-in.-thick baffles and is 75% open. We assumed that the baffles of both silencers are filled with 6-lb/ft^3 density rockwool (a standard industrial practice), which at this density has a specific flow resistance of 760 mks rayls/in., and computed the sound attenuation of each configuration. Figure 13 shows the geometry, together with the predicted sound attenuation vs frequency curves. These theoretical predictions will be checked by scale-model experiments.

At mid and high frequencies, the silencer attenuation is about 10 dB, which matches the sound attenuation of the untreated return leg of the tunnel (see Fig. 3). Consequently, either of the two silencer configurations would result in an optimum overall reduction of the fan noise in the test section. Overall noise reductions in excess of 10 dB would require (1) a more effective silencer upstream of the fan and (2) added sound absorption or silencers in the return leg.

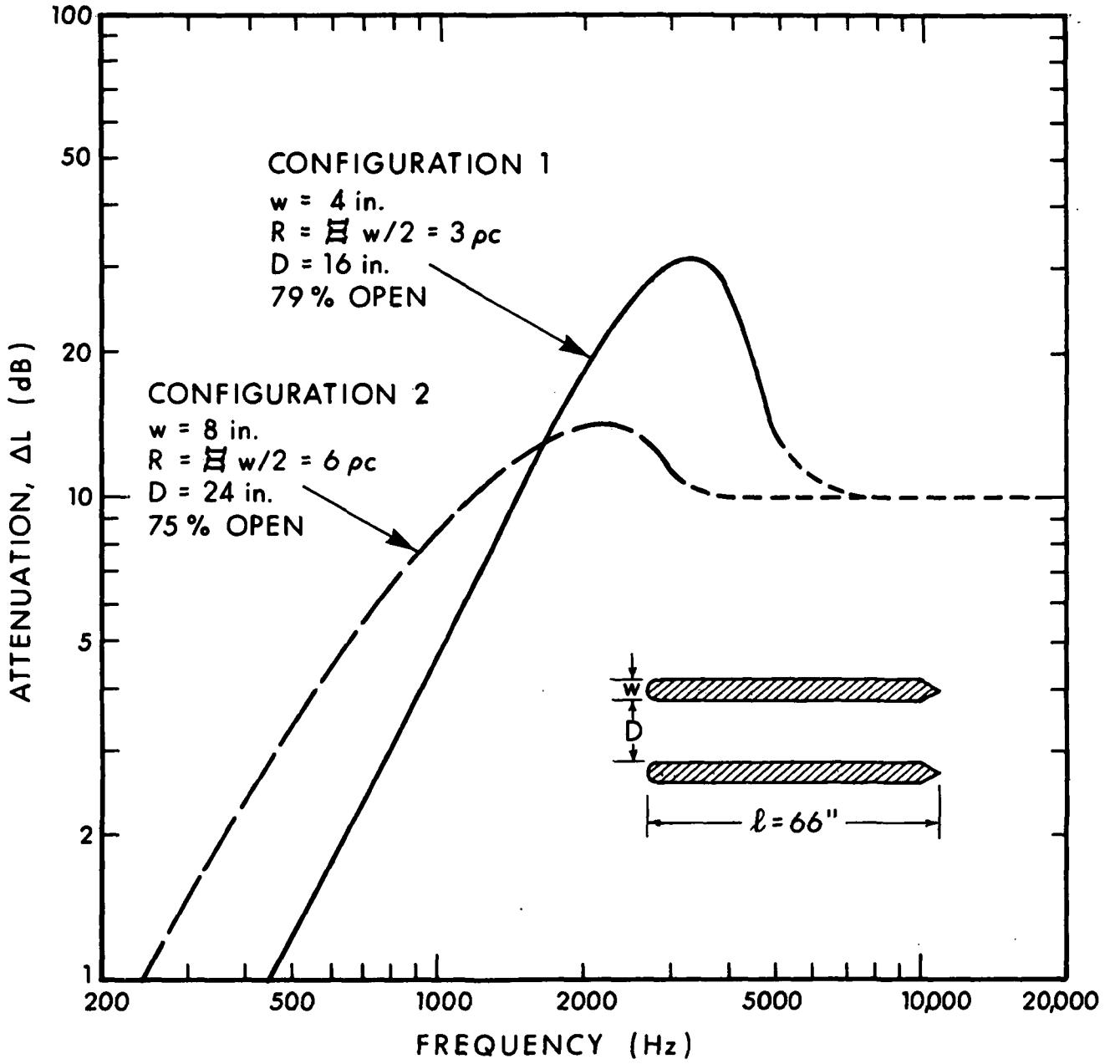

FIG. 13. PREDICTED SOUND ATTENUATION OF THE TWO SILENCER CONFIGURATIONS.

6. CONFIGURATIONS RECOMMENDED FOR SCALE-MODEL TEST

This section includes information pertinent to the design and manufacturing of the scale-model test configurations and a list of the configurations that we recommend you consider for model testing.

6.1 Verification of Scaling

Before the design and manufacturing of the various modified components can be undertaken, it must be demonstrated that the model tunnel scales both the aerodynamics and the acoustics of the full-scale tunnel reasonably well. These tests should be performed as soon as possible, if they have not already been completed.

6.1.1 Aerodynamic scaling

To check the aerodynamic scaling, the following experiments should be carried out:

1. Explore the inflow conditions by tuft probes
2. Measure velocity profiles upstream of the fan at a tunnel speed corresponding to Tunnel Point (TP) 10
3. Measure turbulence spectra upstream of the fan at a tunnel speed corresponding to TP 10
4. Measure the mechanical power of the fan as a function of tunnel speed.

6.1.2 Acoustic scaling

To check the acoustic scaling, the following experiments are required:

1. Measure the 1/3-octave band spectrum of the fan noise in test section at three various tunnel speeds.
2. Evaluate the transfer function between the sound power output of a source (e.g., BBN crossing jet source) of known sound power output located near the propellers and the spectrum of the sound pressure produced by this source in the test section.

6.2 Scale-Model Silencers

Inserting a silencer into the collector duct upstream of the fan can reduce the fan noise in the tunnel test section two ways: (1) The silencer attenuates the noise produced by the fan, and (2) the presence of the silencer improves the inflow conditions to the fan and thereby changes its sound power output. To separate these two effects, we recommend that two geometrically identical baffle configurations should be tested. The first set of baffles should be made of wood and should provide only guidance to the inflow, while the second set should be an acoustic scale model of the full-scale silencer. The proposed construction of the parallel baffles is shown in Fig. 14. The vertically oriented parallel baffles should be inserted into the collector duct upstream of the fan at a distance corresponding to approximately 45 ft at full scale. In the following sections, we discuss configurations that should be considered for model testing.

6.2.1 Solid nonabsorptive baffles

Insert wooden baffles upstream of the fans. With these baffles in place and at an air speed corresponding to TP 10, measure the following quantities:

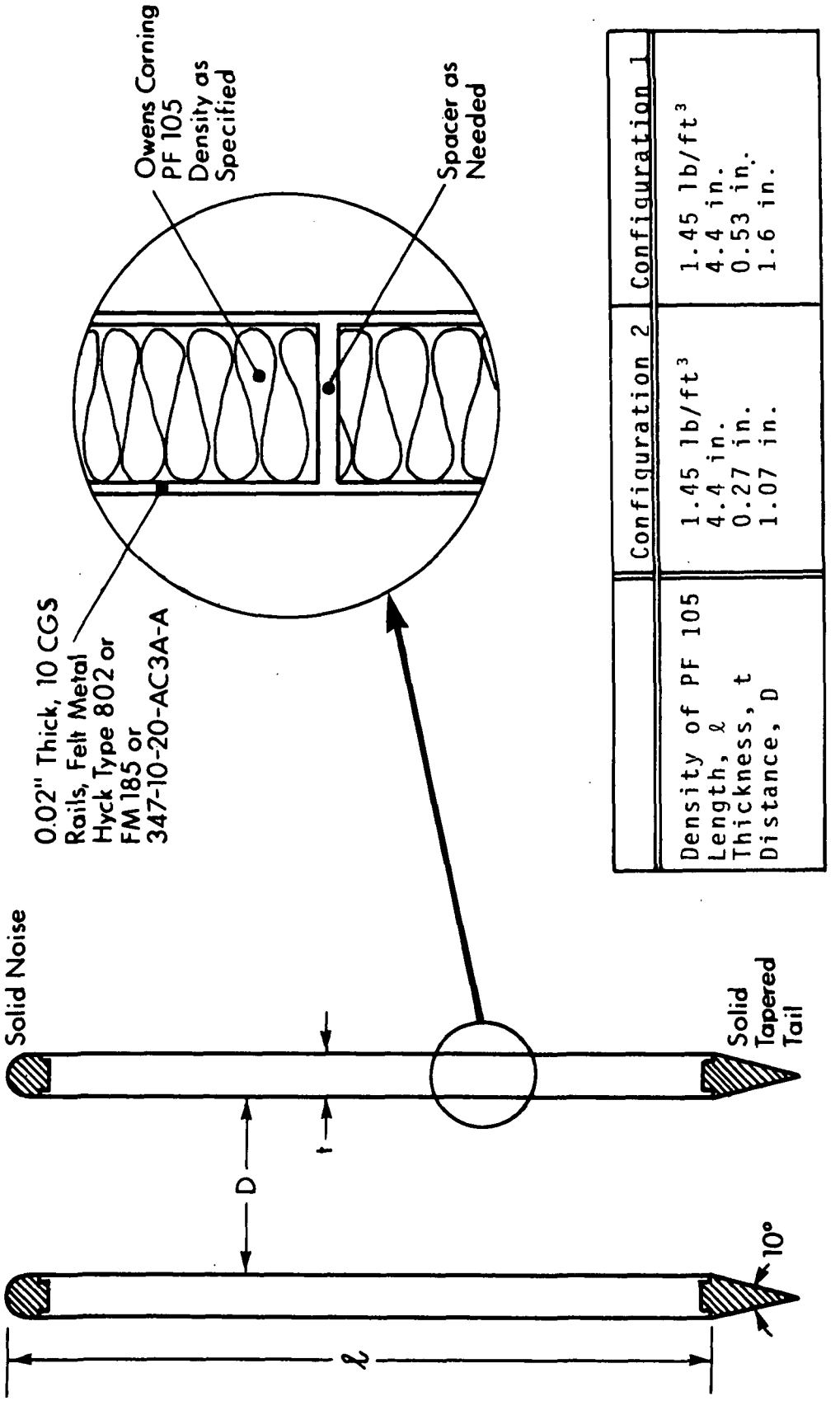

	Configuration 2	Configuration 1
Density of PF 105	1.45 lb/ft³	1.45 lb/ft³
Length, ℓ	4.4 in.	4.4 in.
Thickness, t	0.27 in.	0.53 in.
Distance, D	1.07 in.	1.6 in.

FIG. 14. CONSTRUCTION DETAILS FOR THE SCALE-MODEL DISSIPATIVE SILENCERS.

1. Velocity profile in front of the fan
2. Pressure drop across the silencer
3. Mechanical power input to fan needed to produce the specified air speed
4. Spectrum of the fan noise in the test section.

6.2.2 Screens and honeycomb

To evaluate the effect of devices which break down the vortices generated by the silencer baffles, successively insert a wire mesh screen and a honeycomb just downstream of the solid baffles and repeat measurements (1) through (4), listed in Sec. 6.2.1. The screen should be made of approximately 0.001-in. diameter wire and should be approximately 80% open. The honeycomb should be of 1/2-in. cell or smaller and should be 3 in. to 4 in. long.

6.2.3 Dissipative silencer baffles

The dissipative silencer baffles, as shown in Fig. 14, should be inserted into the collector duct to evaluate their acoustical performance. The following measurements should be made at an air speed corresponding to TP 10:

1. Spectrum of the fan noise in the test section
2. Pressure drop across the silencer.

The results of these tests should be compared with those obtained during the test series of Sec. 6.2.1.

6.3 Platform Modifications

The effect of the test platform on the noise generated by the fan should be studied by modifying and removing the test platform.

6.3.1 Model test platform removed

For an air speed corresponding to TP 10, the following tests should be made:

1. Noise spectrum in the test section
2. Velocity profile upstream of the propeller
3. Mechanical power input to the fans
4. Observe and photograph tuft patterns.

6.3.2 Platform with curved trailing edge

To evaluate whether the inflow distortion – and thereby the noise output of the fan – can be reduced by appropriate shaping of the trailing edge of the test platform, the model test platform should be provided with a curved trailing edge of the largest practicable radius of curvature to assure that the flow remains attached to it. With this modified test platform in place, and at a speed corresponding to Tunnel Point 10, measure the:

1. Noise spectrum in the test section
2. Velocity profile upstream of the propeller
3. Mechanical power input to the fans, and
4. Observe and photograph tuft patterns.

6.4 Blade Modifications

The modifications to the model fan blades, such as adding surface roughness, sharpening the trailing edge, adding a porous trailing edge and sweeping the blade should be tested under two inflow conditions. The conditions are (1) under idealized inflow obtained by removing the model test platform and opening the side doors on the model test section, and (2) under normal conditions with the platform in place and the doors closed. The following quantities should be measured for three different airspeeds:

1. Noise spectrum in the test section
2. Mechanical power input to the fan
3. Pressure rise across the fan.

The blade modifications to be considered for the model test are described below.

6.4.1 Unmodified blades

The unmodified model fan blades should be tested to provide a base for comparison for the performance of the modified blades.

6.4.2 Surface roughness

There is evidence that adding roughness to the propeller blades can reduce the propeller noise. To test the effect of this added surface roughness, we should have available rough grain sandpaper with double-faced adhesive tape ready to be attached to the model blades. The grain size should be comparable to the boundary layer thickness.

6.4.3 Sharpened trailing edge

Sharpening the trailing edge of the fan blades pushes the peak frequency of vortex shedding noise up to higher frequencies where the fan noise suffers higher attenuation along its path from the fan to the test section. To evaluate experimentally the effect of this modification on the fan noise in the test section, a set of the unmodified model propellers should be formed to accept an add-on sharp trailing edge. A possible method of adding the sharp trailing edge to the blade is shown in Fig. 15. The trailing edge should be made as sharp as practicable.

6.4.4 Porous trailing edge

Adding a porous trailing edge to the propellers can substantially reduce the trailing edge boundary layer noise and virtually eliminate the trailing edge vortex noise [5]. The data presented in Fig. 16 show the effect of such a porous edge on the noise radiated by the trailing edge of a 1/4-in.-thick plate.

The porous edge can be made of 0.02-in.-thick wire mesh enforced fiber metal of 10 cgs rayls flow resistance. A possible method of attachment is shown in Fig. 15.

6.4.5 Blade sweep

The tip region contributes most to fan noise because it is the area of highest relative speed between the air and the blade. Sweeping the blade near the tip region helps to reduce fan noise. The sweep of the leading edge reduces turbulence ingestion noise by minimizing the net dynamic force on the blade, while the sweeping trailing edge results in a reduction of the trailing edge vortex noise by reducing the coherence of the vortex shedding along the edge. Typical blade sweep geometries are shown in Fig. 17.

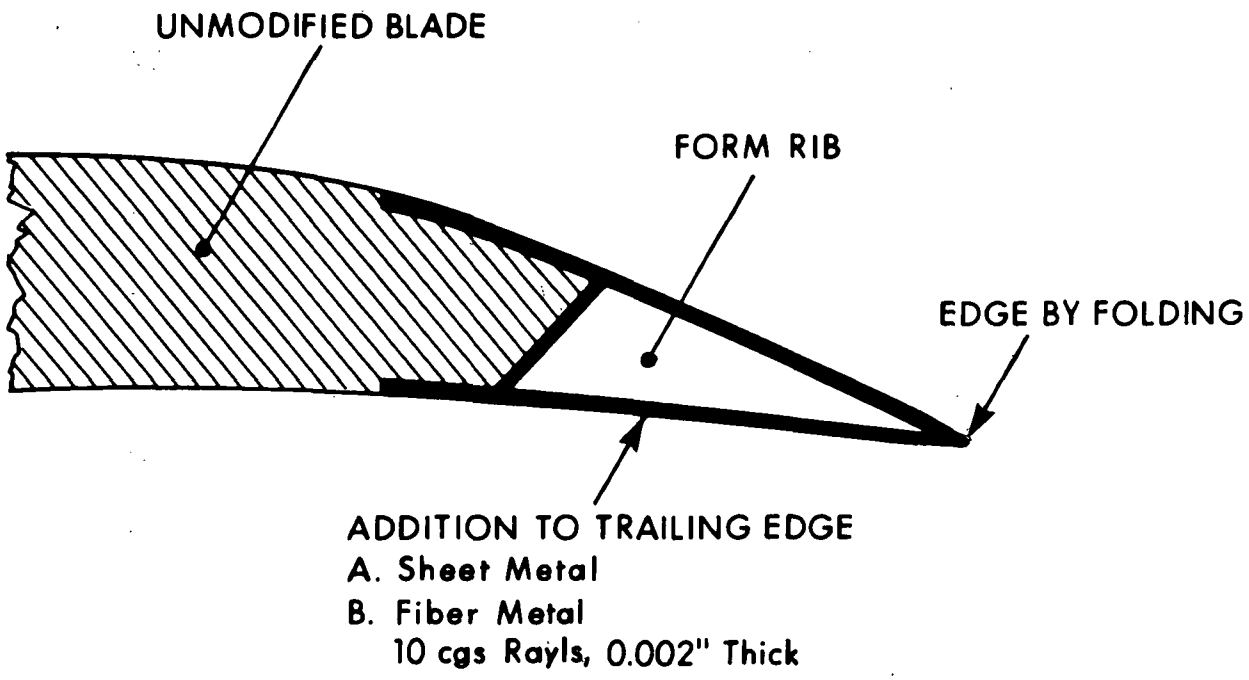

FIG. 15. POSSIBLE METHOD OF ATTACHMENT OF TRAILING EDGE MODIFICATIONS.

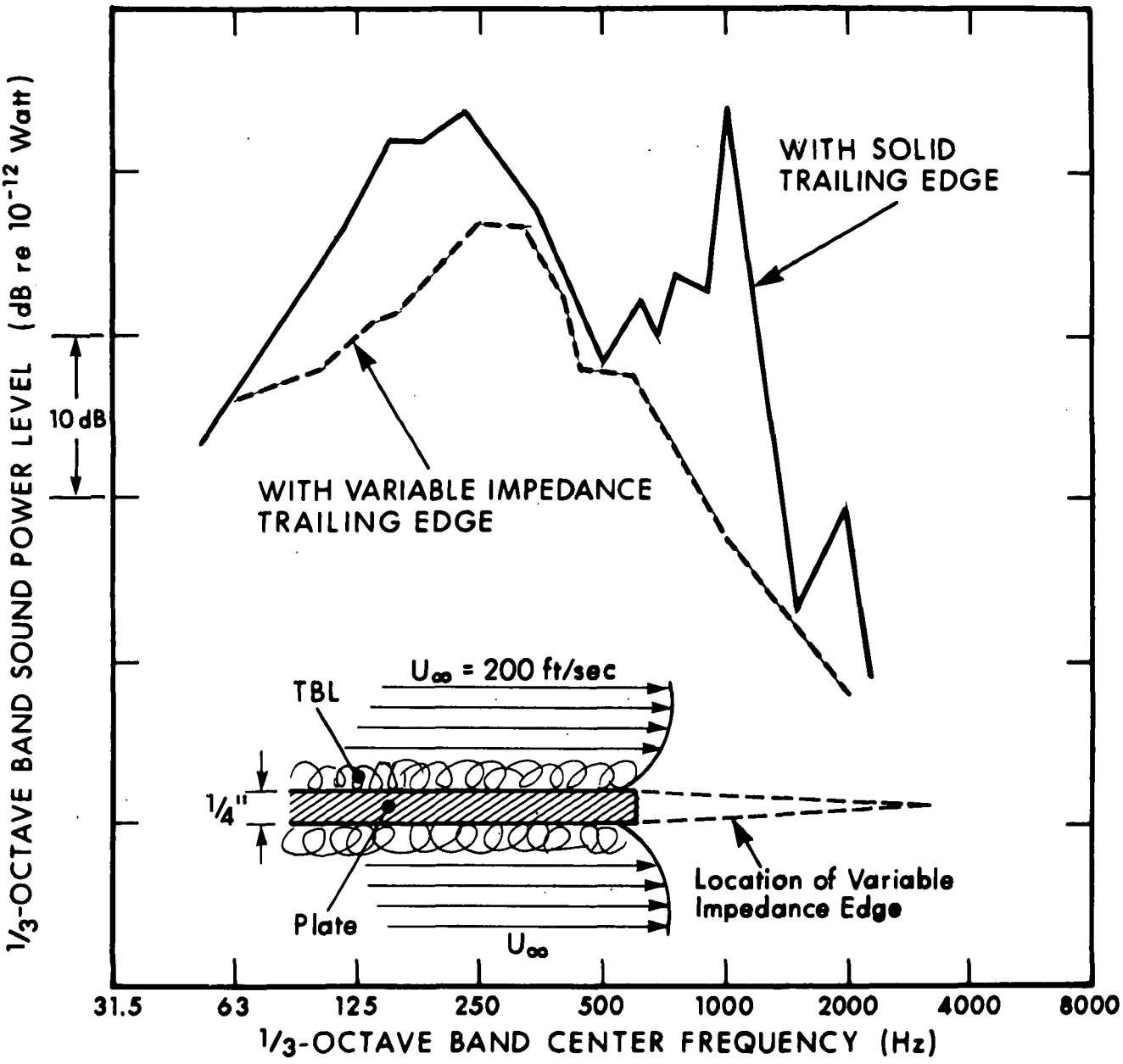

FIG. 16. EFFECT OF A POROUS TRAILING EDGE ON TRAILING EDGE NOISE.

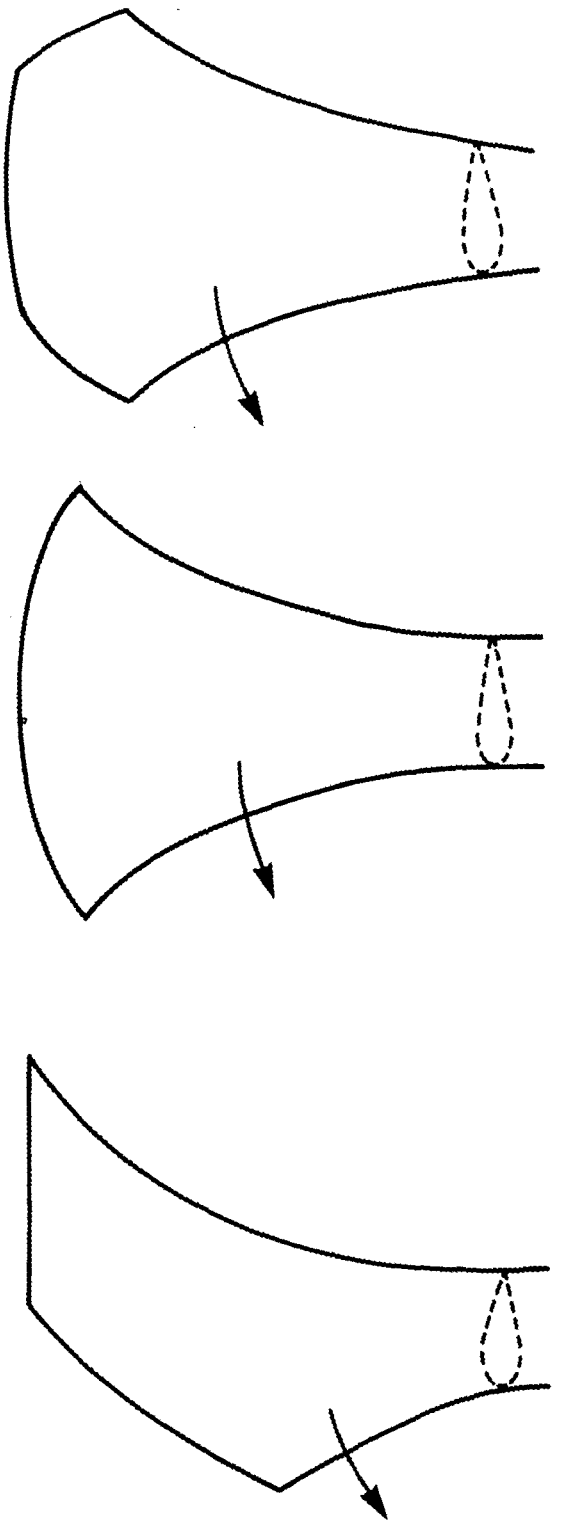

FIG. 17. TYPICAL BLADE SWEEP CONFIGURATIONS.

In designing the sweeping tip of the blades, the following constraints should be kept in mind:

- The lift distribution vs radius of the swept blade should be the same as that of the unmodified blade. Because the swept blade has a larger surface, its lift coefficient must be reduced appropriately by lowering the angle of attack.
- The locus of the centers of gravity of the blade sections should be arranged so as to minimize in-plane bending moments, especially near the hub.
- Laws of aerodynamic centers should be arranged to minimize blade twist.
- The distribution of the angle of attack with radius should take into account the radial distribution of the inflow velocity. Such an angle of attack distribution may increase the efficiency of the propellers and thereby help to reduce further the noise output for a given tunnel speed.

The theoretical reduction in sound power level caused by the blade sweep is given by:

$$\Delta PWL_L \simeq 30 \log (\cos \Lambda)$$

$$\Delta PWL_T \simeq 50 \log (\cos \Lambda) \quad ,$$

where ΔPWL_L and ΔPWL_T is the reduction in sound power level in dB of the leading edge and trailing edge vortex noise, respectively, and Λ is the sweep angle (i.e., the angle from the radial). Accordingly, a 45° sweep angle results in an approximate 5-dB reduction of the turbulence ingestion noise and a 9-dB reduction in the trailing edge vortex noise. Preferably, sweep angle is distributed along the radius to emphasize the tip region where

the relative airspeed is the highest. Figure 18 shows two preferred sweep angle vs radius curves (these should not be confused with the geometry of the edge) for the full-scale blades. The sweep is concentrated at the tip region where the blade operates in the turbulent shear layer. The sweep is chosen to be symmetrical for the leading and trailing edge to avoid structure problems. For evaluation, the selected scale-model propeller, equipped with sweeping tips for its acoustical and aerodynamical performance, should be tested under two inflow conditions: (1) under idealized inflow conditions obtained by removing the model test platform and opening the side doors of the model test section, and (2) under normal conditions with the model test platform in place and the doors closed. The following measurements should be made for three different air speeds:

- Noise spectrum in the test section
- Mechanical power input to the fan
- Pressure rise across the fan.

6.5 Other Tunnel Modifications

The fan noise may be reduced by reducing the thickness of the shear layer in the inflow to the fans or by allowing the outer annulus of flow, which contains the shear layer, to bypass the fan completely. These modifications would require considerable redesigning of the collector and drive section of the tunnel; they are discussed in Appendix B.

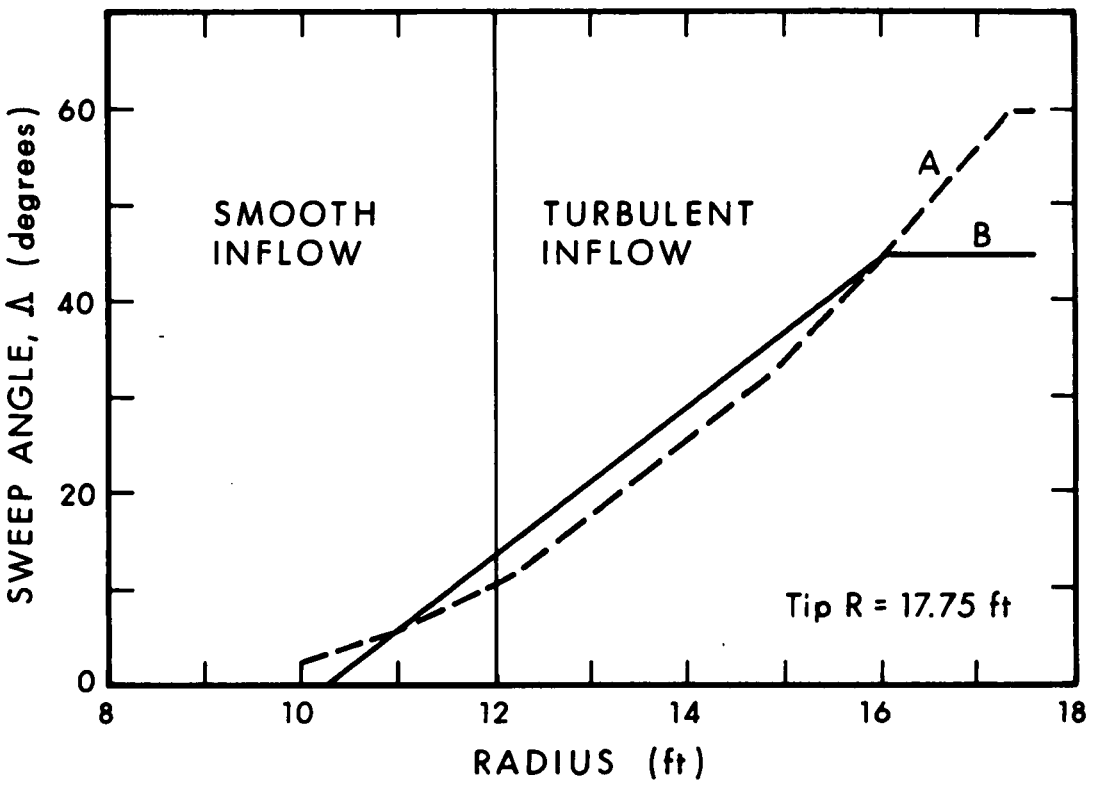

FIG. 18. DISTRIBUTION OF SWEEP ANGLE ALONG THE RADIUS
A) Linearly Increasing
B) Exponentially Increasing

REFERENCES

1. Vér, I.L., Malme, C.I., and Meyer, E.B., "Acoustical Evaluation of the NASA Langley Full-Scale Wind Tunnel," BBN Report No. 2100, NAS1-9559 (1971).

2. Vér, I.L., "Acoustical Modeling of the Test Section of the NASA Langley Research Center's Full-Scale Wind Tunnel," BBN Report No. 2280, NAS1-9559 (1971).

3. Hayden, R.E., Kadman, Y., and Africk, S., "An Approach to Detailed Diagnostic Calculations of Airframe Noise," BBN Report No. 2791 (1974).

4. Private communications with Dr. James Sheiman of NASA Langley.

5. Hayden, R.E. and Shanoud, R., "Method of and Structures for Reducing Sound Generation in Fluid Flow Systems Embodying Foil Structures and the Like," U.S. Patent 221,223 (1972).

APPENDIX A: SUMMARY OF SILENCER PRESSURE DROP CALCULATIONS

The drag coefficient of a single streamlined silencer panel has been measured by NASA.* The pertinent aerodynamic properties of the panel were:

Surface Area (one side)	$S_0 = 29.1\ ft^2$
Edge Length (facing the flow)	$\ell_0 = 5.58\ ft$
Baffle Width	$w = 0.33\ ft$
Drag Coefficient	$C_D = 0.0152$

The pressure drop across the silencer is given by:

$$\Delta p = \frac{D_L}{A} \quad , \tag{1}$$

where D_L is the total drag force on all silencer panels and A is the total silencer face area (i.e., the cross-sectional area of the collector upstream of the fans).

The total drag force for unit edge length is:

$$D_1 = C_D S_0 \frac{1}{\ell_0} q_s \quad , \tag{2}$$

where q_s is the dynamic pressure head in the silencer passage. For a total silencer edge length of L, the total drag force is then:

$$D_L = C_D S_0 \frac{L}{\ell_0} q_s \quad . \tag{3}$$

---

*Private communications with Dr. James Sheiman of NASA.

Combining Eqs. 1 and 3 yields the pressure drop across the silencer:

$$\Delta p = C_D \frac{S_0}{A} \frac{L}{\ell_0} q_s \quad . \tag{4}$$

The dynamic pressure head in the silencer passage is related to the dynamic pressure head in the test section q_t as:

$$q_s = q_t \left(1 - \frac{wL}{A}\right)^{-2} \simeq q_t \left(1 - 2w \frac{L}{A}\right)^{-1} \quad . \tag{5}$$

Combining Eqs. 4 and 5 and considering that the maximum permissible pressure drop across the silencer is approximately $\Delta p_{max} \simeq 0.08\ q_t$, one obtains:

$$0.08 = C_D \frac{S_0}{A} \frac{L}{\ell_0} \left(1 - 2w \frac{L}{A}\right)^{-1} \quad . \tag{6}$$

Solving Eq. 6 for L yields:

$$L = \frac{A}{2w + \dfrac{C_D\ S_0}{0.08\ \ell_0}} \quad . \tag{7}$$

Now, considering that the percentage open area, POA, of the silencer made up of parallel baffles of width w is:

$$POA = 100 \left(1 - \frac{wL}{A}\right) \quad , \tag{8}$$

and solving Eq. 8 for L and inserting this value of L into Eq. 7 yields the minimum percentage open area required so that the pressure drop across the silencers does not exceed the maximum permissible pressure drop of $\Delta p_{max} = 0.08\ q_t$:

$$POA_{min} \simeq 100 \left(1 - \frac{1}{2 + \frac{C_D S_0}{0.08 \ell_0 w}} \right) . \quad (9)$$

Solving Eq. 9 for $S_0 = 29.1$ ft^2, $\ell_0 = 5.58$ ft, $w = 0.33$ ft and $C_D = 0.0152$ yields:

$$POA_{min} \simeq 100 \left(1 - \frac{1}{2 + \frac{0.0152 \times 29.1}{0.08 \times 5.58 \times 0.33}} \right) = 80\% .$$

With baffles of thickness w, the distance between the faces of two neighboring baffles D is given by:

$$D = w \frac{POA/100}{1 - \frac{POA}{100}} . \quad (10)$$

Solving Eq. 10 for w = 4 in. and POA = 80 yields:

$$D = 4 \text{ in.} \frac{0.8}{1 - 0.8} = 16 \text{ in.} .$$

Accordingly, the on-center spacing of the 4-in.-thick baffles is 16 in. + 4 in. = 20 in.

APPENDIX B: REDUCTION OR ELIMINATION OF THE SHEAR LAYER

The fan noise may be reduced by reducing the thickness and turbulence of the shear layer in the inflow or by completely by-passing the outer annulus of flow. Tunnel modifications which would be required to achieve this reduction are discussed below.

B.1 Optimum Collector Cowl Design

Since the tunnel test section is not vented, the conservation of mass requires that in steady state the same amount of air that enters the test section through the nozzle must exit from it through the collector duct. However, the free jet mixes with the stationary air in the test section and entrains air into the shear layer. This entrained air must be returned to the test section at the stagnation point on the collector cowl by steady circulation or by unsteady processes. *The requirement to maintain a mass flow balance makes it inevitable that a part of the turbulent shear layer is "swallowed" by the cowl. This happens, regardless of the cowl shape, in all unvented test sections.*

However, one should make sure that no additional turbulence is generated during this ingestion process by designing a collector cowl which provides as steady a stagnation process on the cowl as possible. If a steady stagnation process is not possible, then the mass flow balance can be maintained only through an unsteady process at the cowl, resulting in the generation of additional turbulence and thus, higher fan noise output. *Accordingly, the design of the collector cowl should be optimized to minimize the amount of the excess turbulence.* In addition to the possible fan noise reduction, an optimized collector cowl design would also result in a more steady mean flow in the tunnel test section and in lower noise levels because of a flow-solid-body interaction at the collector cowl.

B.2 Favorable Pressure Gradient

The turbulence levels at the fan can be reduced by providing a favorable pressure gradient (which enhances turbulence decay) all the way from the cowl to the fan. This gradient can be achieved by reducing the cross-sectional area of the collector duct continually up to the fan plane. (See Fig. 19 for possible configuraton.)

At this time, we do not know the exact extent of the net effect of such a change on the fan noise, or whether the higher mean flow to the fan required to achieve the same air speed in the test section will partially offset the advantages of a reduced turbulence level. Therefore, we urge you to study such a change to determine if it is feasible in terms of its aerodynamic consequences and the extent of structural changes required. However, we would like to note that the type of collector modifications required to reduce the collector throat area is usually compatible with the modifications required to help stabilize the shear layer attachment at the collector cowl.

B.3 Shear Layer By-Pass

With the drive section geometry shown schematically in Fig. 20, the entire shear layer can be made to by-pass the fan blades. This measure is analogous to venting the test section. To "drive" the by-passing flow, the static pressure across the by-pass duct $p = p_{in} - p_{out}$ must balance the losses of the by-pass duct. Since the static pressure increases across the fan, the downstream passage must converge significantly to lower the static pressure sufficiently at the downstream end of the by-pass. We recommend that you explore whether or not such a by-pass could be implemented without major structural changes and without considerable loss of aerodynamic performance.

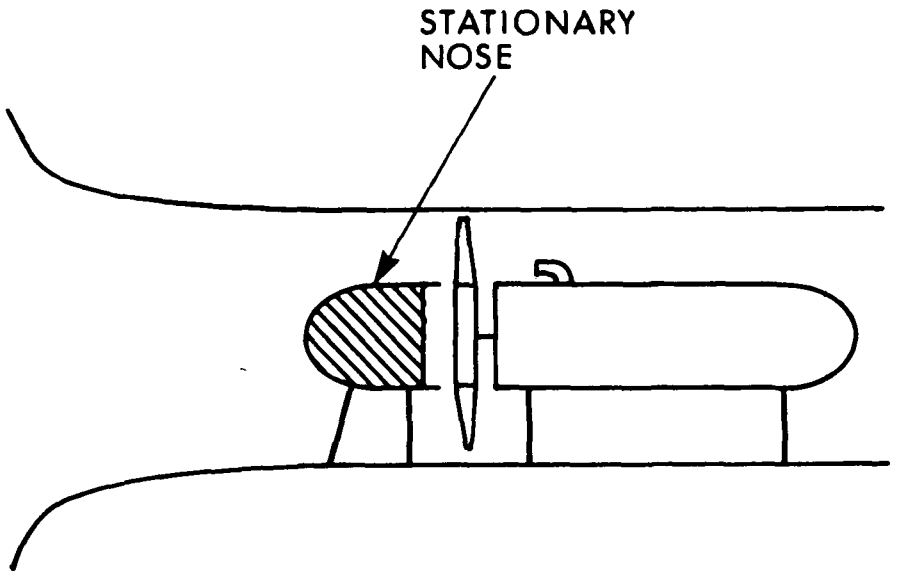

FIG. 19. DECREASED COLLECTOR DUCT CROSS-SECTION TO YIELD FAVORABLE PRESSURE GRADIENTS REDUCING INFLOW TURBULENCE.

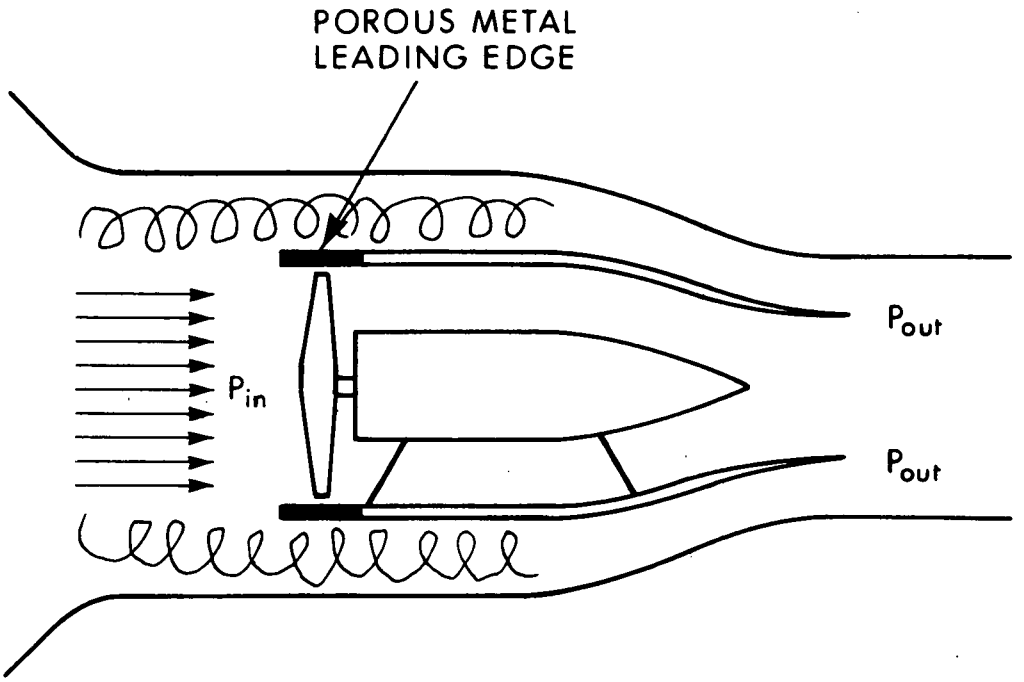

FIG. 20. BY-PASS THE INGESTED SHEAR LAYER.